Developmental Biology 394 (2014) 340–356

Contents lists available at ScienceDirect

Developmental Biology

journal homepage: www.elsevier.com/locate/developmentalbiology

FAK is required for tension-dependent organization of collective cell movements in *Xenopus* mesendoderm

Maureen A. Bjerke, Bette J. Dzamba, Chong Wang, Douglas W. DeSimone *

Department of Cell Biology, School of Medicine, University of Virginia Health System, P.O.Box 800732, Charlottesville, VA 22908, USA

ARTICLE INFO

Article history:
Received 7 February 2014
Received in revised form
4 July 2014
Accepted 30 July 2014
Available online 13 August 2014

Keywords:
Focal adhesion kinase
Keratin
Integrin
Cadherin
Gastrulation
Cell migration

ABSTRACT

Collective cell movements are integral to biological processes such as embryonic development and wound healing and also have a prominent role in some metastatic cancers. In migrating *Xenopus* mesendoderm, traction forces are generated by cells through integrin-based adhesions and tension transmitted across cadherin adhesions. This is accompanied by assembly of a mechanoresponsive cadherin adhesion complex containing keratin intermediate filaments and the catenin-family member plakoglobin. We demonstrate that focal adhesion kinase (FAK), a major component of integrin adhesion complexes, is required for normal morphogenesis at gastrulation, closure of the anterior neural tube, axial elongation and somitogenesis. Depletion of zygotically expressed FAK results in disruption of mesendoderm tissue polarity similar to that observed when expression of keratin or plakoglobin is inhibited. Both individual and collective migrations of mesendoderm cells from FAK depleted embryos are slowed, cell protrusions are disordered, and cell spreading and traction forces are decreased. Additionally, keratin filaments fail to organize at the rear of cells in the tissue and association of plakoglobin with cadherin is diminished. These findings suggest that FAK is required for the tension-dependent assembly of the cadherin adhesion complex that guides collective mesendoderm migration, perhaps by modulating the dynamic balance of substrate traction forces and cell cohesion needed to establish cell polarity.

Introduction

The morphogenetic events of early embryonic development are comprised of a series of complex cell and tissue movements. These movements include mesendoderm migration, epiboly and convergent extension, each of which relies on tight temporal and spatial control of chemical and mechanical signals over multiple length scales (Keller et al., 2000; Shook and Keller, 2003; Winklbauer, 2009). Developing embryos can be considered morphogenetic machines, generating and responding to a variety of forces including compression, traction, tension, and flow (Wozniak and Chen, 2009). In recent years there has been a growing appreciation for the importance of the mechanical properties of the developing embryo, particularly in the case of tension-dependent signaling through adhesion receptors (Keller, 2012; Schwartz and DeSimone, 2008).

Xenopus mesendoderm provides a striking example of cells migrating cooperatively as a cohesive unit. Mesendoderm cells move collectively at gastrulation across a fibrillar fibronectin (Fn) matrix lining the roof of the blastocoel cavity (Winklbauer, 2009), generating traction forces on the substrate as they proceed (Davidson et al., 2002). Cohesion of the mesendoderm tissue is maintained by cadherin-based cell–cell contacts across which tensile forces are distributed (Davidson et al., 2002; Lee and Gumbiner, 1995). Tension on C-cadherin is sufficient to direct polarized protrusive activity, assembly of junctional complexes containing catenin-family proteins, and rearrangement of the keratin intermediate filament cytoskeleton (Weber et al., 2012). These responses are dependent on adhesion of mesendoderm cells to a Fn substrate. The interaction of cells with the Fn matrix through integrin adhesion complexes is also essential for other morphogenetic movements during gastrulation, including epiboly and convergent extension (Davidson et al., 2006, 2002; Marsden and DeSimone, 2003, 2001).

Focal adhesion kinase (FAK) is a non-receptor tyrosine kinase that is a central component of integrin adhesion complexes. FAK was originally identified as a highly phosphorylated protein that localizes to integrin adhesion complexes (Hanks et al., 1992; Schaller et al., 1992) and is activated by adhesion to extracellular matrix (ECM) and clustering of integrins (Calalb et al., 1995). The kinase activity of FAK is regulated via phosphorylation of conserved tyrosine residues in response to adhesion, growth factor

* Corresponding author.
E-mail address: desimone@virginia.edu (D.W. DeSimone).

http://dx.doi.org/10.1016/j.ydbio.2014.07.023
0012-1606/

signaling and other extracellular stimuli (Mitra et al., 2005). Signaling by FAK through downstream effector proteins influences cell survival, growth, adhesion and motility (Parsons, 2003). FAK is essential for the normal adhesion and migration of many cell types both in vitro and in vivo (Ilić et al., 1995; Mitra et al., 2005). Cell culture studies have also demonstrated that FAK expression and activity impact the organization and polarity of cells undergoing directed migration (Gu et al., 1999; Lim et al., 2010; Owen et al., 2007; Schober et al., 2007; Tomar et al., 2009; Wang et al., 2001), however, the mechanism of these actions is not well understood.

While FAK is typically localized to integrin adhesions, it has been reported in some cases to be enriched at cell–cell contacts (Crawford et al., 2003; Playford et al., 2008), suggesting a potential role in integrin–cadherin crosstalk. FAK can influence the stability of cell–cell adhesions indirectly by stimulating expression of E-cadherin (Wang et al., 2004) or by modulating Rho activity (Playford et al., 2008). FAK is also thought to regulate assembly and disassembly of integrin adhesion complexes (Mitra et al., 2005) and to be critical for sensing and regulating changes in integrin-dependent adhesion forces (Dumbauld et al., 2010; Schober et al., 2007; Wang et al., 2001). Therefore, FAK is likely to be an essential element of an adhesive network that integrates chemical and mechanical cues to regulate collective movements in developing embryos and tissues (Weber et al., 2011).

Several loss-of-function studies have implicated FAK in the normal development of *Xenopus* and other vertebrate models (Crawford et al., 2003; Doherty et al., 2010; Fonar et al., 2011; Furuta et al., 1995; Henry et al., 2001; Ilić et al., 1995; Kragtorp and Miller, 2006; Petridou et al., 2013, 2012; Stylianou and Skourides, 2009). Although most studies have focused on late stages of development, targeted disruption of the FAK gene in mice revealed defects in gastrulation and morphogenesis of mesodermal derivatives (Furuta et al., 1995). FAK knockout embryos show no obvious defects in mesoderm differentiation and are able to initiate gastrulation but they fail to separate the three germ layers and do not survive beyond the end of neurulation. In *Xenopus* embryos, FAK expression increases during gastrulation (Hens and DeSimone, 1995) and is enriched in the mesoderm, mesendoderm, and ectoderm (Petridou et al., 2012). Recent investigations using dominant negative constructs (Kragtorp and Miller, 2006; Petridou et al., 2013; Stylianou and Skourides, 2009) or antisense inhibition of FAK expression (Fonar et al., 2011) have implicated FAK in neurulation, axial elongation and somitogenesis. However, these studies include a number of discrepant observations, perhaps reflecting variations in the approaches and assays used and/or the developmental stages investigated. Although there is some indication that FAK is important for normal migration of mesendoderm cells (Stylianou and Skourides, 2009), little is known about specific FAK functions at gastrulation or the role of FAK in responding to and regulating mechanical signals during this process.

In the current study we investigate the contributions of FAK to morphogenetic movements in early stage embryos and, in particular, the role of FAK in the tension-dependent organization of collectively migrating mesendoderm. Detailed analyses of single cell behaviors are essential to understanding the emergent properties of a tissue undergoing collective movements, for example, the mediolateral intercalation of cells that drives convergent extension and axial elongation (Keller, 2002). The *Xenopus* embryo is particularly advantageous for analyses of complex behaviors of cells and tissues. Mesendoderm explanted from the embryo recapitulates the in vivo behavior of the developing tissue and is amenable to imaging and manipulation (Davidson et al., 2002). We use explants in combination with biochemical and biophysical techniques to establish the role of FAK in the collective migration of the mesendoderm tissue during gastrulation.

Materials and methods

Xenopus embryos, animal caps and Keller sandwiches

Xenopus laevis embryos were obtained using standard methods, cultured in 0.1 × Modified Barth's Saline (MBS; Sive et al., 2000) and staged according to Nieuwkoop and Faber (1994). Animal cap extension assays were performed as previously described (Symes and Smith, 1987) except with 5 ng/mL recombinant activin (R&D Systems) as the inducing signal. Keller sandwiches were prepared as described in Sive et al. (2000), with minor modifications. Briefly, the dorsal marginal regions of two control or two FAK morphant embryos were dissected and then sandwiched together such that the ectoderm faced outward. The sandwiches were compressed lightly between coverglass and a clay bottomed dish for 60 min, then uncovered and incubated in 0.5 × MBS until stage matched embryos had completed axial elongation.

Morpholinos

The antisense morpholino oligodeoxynucleotide (MO) used to inhibit translation of FAK mRNA was obtained from Gene Tools (Philomath, OR). The FAK MO (5′-CAGGTAAGCCGCAGCCATAGCCTTG-3′) corresponds to a region that includes the translation start site and is complementary to the published *X. laevis* and *X. tropicalis* cDNA sequences for FAK (NM_001090597.1 and CR926269.1). FAK MO contains 2 mismatches with the putative pseudoallele of FAK in *X. laevis* (NM_001091540.1). The standard GeneTools Control MO sequence (5′ CCTCTTACCTCAGTTACAATTTATA 3′) was used in all control experiments. Morpholinos were injected into 1 or 2-cell stage embryos at a final concentration of 20–25 ng per embryo. Alexa–dextrans (Invitrogen) were co-injected with morpholinos to allow sorting of MO injected embryos (morphants) and to facilitate tracking of cell movements and analyses of cell shape.

RNA constructs

For expression of fluorescently-tagged proteins and of FAK constructs, RNA was transcribed in vitro from plasmid DNA templates. The following constructs were used in this study: pCS2 GAP43-EGFP (E. DeRobertis, University of California), pCS107 GFP–moesin (J. Wallingford, University of Texas), EGFP-XCK1(8) (V. Allan, University of Manchester; Clarke and Allan, 2003), pCS2 xFAK (subcloned using fragments B1 and F1 from Hens and Desimone, 1995), and pCS2 cFAK (J.T. Parsons, University of Virginia). Constructs used for imaging mesendoderm explants (GAP43-EGFP, GFP–moesin, and EGFP-XCK1(8)) were injected into the marginal zone region of one or both dorsal blastomeres at the 4-cell stage with a final concentration of 500–700 pg of RNA per embryo. xFAK and cFAK were injected animally into both blastomeres at the 2-cell stage with a final concentration of 200 pg of RNA per embryo.

Microscopy and image analysis

Embryos and explants were photographed on a Zeiss SteREO Lumar.V12 stereomicroscope using a Zeiss AxioCam MRm camera. Widefield fluorescence images were collected using a Zeiss AxioObserver inverted microscope, Zeiss PlanApo/20 × /0.8 and PlanApo/40 × /1.0/Ph3 objectives, Retiga Exi camera (QImaging) and Volocity software (Improvision/PerkinElmer). Structured illumination images were collected on the Zeiss AxioObserver using an OptiGrid system (Qioptic). Confocal images were taken on a Nikon C1 confocal microscope with a Nikon PlanApo/60 × /1.40 objective. Image analysis was performed using Volocity, ImageJ (http://rsb.info.nih.gov;

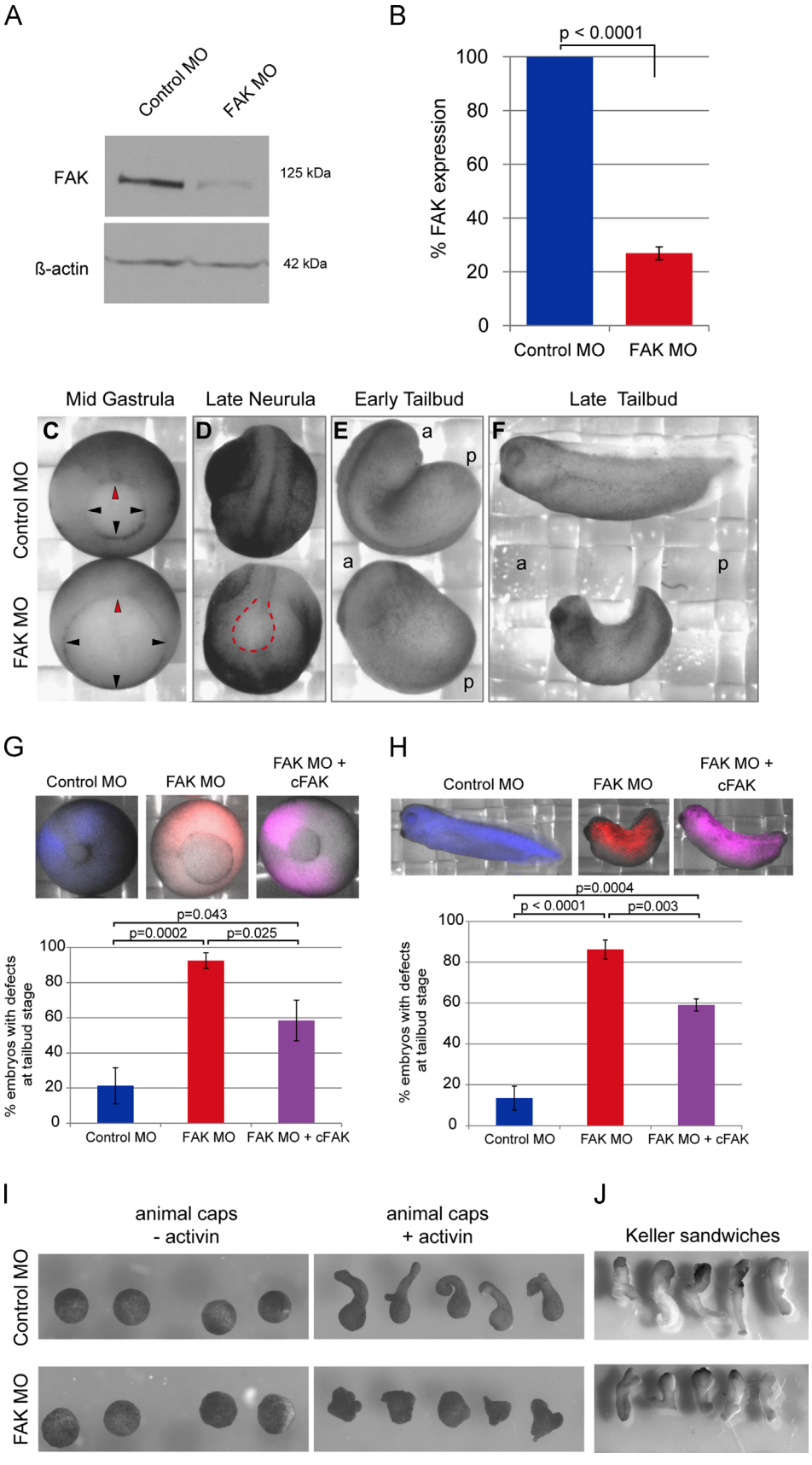
A
Control MO
FAK MO
FAK
125 kDa
ß-actin
42 kDa
B
p < 0.0001
% FAK expression
100
80
60
40
20
0
Control MO
FAK MO
Mid Gastrula
Late Neurula
Early Tailbud
Late Tailbud
C
D
E
F
Control MO
FAK MO
a
p
G
Control MO
FAK MO
FAK MO + cFAK
p=0.043
p=0.0002
p=0.025
% embryos with defects at tailbud stage
H
p=0.0004
p < 0.0001
p=0.003
I
animal caps - activin
animal caps + activin
J
Keller sandwiches

National Institutes of Health) and Fiji (http://fiji.sc/Fiji; Schindelin et al., 2012) software packages.

Fixation and immunofluorescence

For imaging of internal structures and staining of animal caps, embryos were fixed in 3.7% formaldehyde overnight at 4 °C. Embryos were washed in 1 × Tris–HCl buffered saline + 0.1% Tween20 (TBS–tween) and sectioned or bisected on a clay-bottomed dish using a scalpel blade. Bisected gastrulae were imaged using a stereomicroscope, tailbud sections were imaged using a confocal microscope. Animal caps were cut from fixed stage 11 embryos and incubated overnight at 4 °C with an antibody directed against Fn (4H2; Ramos et al., 1996), diluted 1:300 in TBS–tween. Caps were washed in TBS–tween and incubated with an Alexa-tagged secondary antibody (Invitrogen) then washed again and mounted in 50% glycerol/TBS. Caps were imaged by structured illumination as described above.

Quantification of cell spreading and migration

Mesendoderm tissue was excised from the leading edge of the mesendoderm mantle of stage 10–11 embryos and dissociated in 1 × Ca^{2+}/Mg^{2+}-free MBS for 40 min. Cells were then plated at a sub-confluent density into 0.5 × MBS on a coverslip coated overnight at 4 °C with 0.39 μg/cm^2 bovine plasma Fn and blocked with 5% bovine serum albumin. Cells were given 1 h to attach and spread and were imaged using brightfield or widefield fluorescence illumination on an inverted microscope. For migration studies, Volocity imaging software was used to acquire time-lapse images every 30 s for 10–20 min. Movements of single cells were tracked using automated identification of cell centroids. Cells in explants were outlined manually but centroid identification and tracking was automated. Average velocity was calculated by dividing final displacement by total elapsed time. Persistence was calculated by dividing total cell path length by final displacement. ImageJ was used for counting spread cells and calculating circularity. Cells were outlined manually and circularity calculated using the Shape Descriptors function.

Mesendoderm explant preparation

Glass coverslips were washed in alkaline-ethanol solution and flamed, and then affixed using epoxy to the bottom of 35 mm plastic dishes previously drilled with a lathe. Coverslips were coated with 200 μL of 2.5 μg/mL bovine plasma Fn (Calbiochem) overnight at 4 °C to yield a coating density of 0.39 μg/cm^2. Coverslips were blocked with 5% bovine serum albumin then washed with 0.5 × MBS. Dorsal marginal zone explants were prepared as previously described (Davidson et al., 2004, 2002). Explants were placed on the Fn coated coverglass or on Fn coated PDMS gels (see Section "Mesendoderm explants" for details of gel preparation), lightly compressed under glass fragments supported by silicone grease, and allowed 1 h to adhere and begin to migrate prior to imaging. Migrating mesendoderm tissue undergoes occasional periods of retraction. To prevent these events from obscuring any differences in migration rate and persistence, migration was quantified during time windows during which no retractions occurred. Migration rate and persistence were measured in the leading row of cells in each explant. The changes in these measures thus reflect changes in the rate of tissue advancement.

Protrusion quantification

Migrating explants expressing GAP43-EGFP were imaged using a Nikon C1 confocal microscope. Six 1 μm z-slices covering the portion of the cells in immediate contact with the Fn substrate were acquired every 30 s for 5–10 min. The last frame of each time-lapse series was used for all analyses, with the earlier time points used to exclude cell–cell interactions and retracting cell extensions from analysis. Yolk-free areas were designated as lamellipodial protrusions and fine filopodial extensions were excluded. Protrusion angles were measured using ImageJ as described previously (Weber et al., 2012) and rose diagrams were plotted in OriginPro 7.5 (OriginLab).

Quantification of traction forces

Single cells

DiI labeled, Fn-coated (by micro-printing to ensure only top of posts are coated), #12 microfabricated post array detectors (mPADs) were obtained from Christopher Chen's lab (Yang et al., 2011). Before use, mPADs were recoated with bovine plasma Fn overnight, then blocked with 5% bovine serum albumin and washed with 0.5 × MBS. Cells isolated from the leading edge of the mesendoderm mantle were plated on prepared mPADs at sub-confluent density. A single-plane confocal image was acquired for each attached cell, capturing both the dextran-labeled cells and the top of the fluorescent microposts. Measurement of the deflection of the posts and force calculations were carried out in Matlab (MathWorks) using a program provided by Mark Breckenridge and the Chen lab.

Mesendoderm explants

The preparation of mesendoderm explants requires compression of the tissue immediately after dissection and this compression step interferes with measurement of micropost deflection. To avoid this complication, an alternate method was used for measurement of traction stresses exerted by cells in mesendoderm explants. Polyacrylamide gels were prepared following a protocol modified from that described by Rajagopalan et al. (2004). Briefly, a mixture containing 6% acrylamide (Fisher Scientific), 0.36% bis-acrylamide

Fig. 1. FAK knockdown inhibits gastrulation movements and axial elongation. (A) Representative Western blot of FAK expression levels in stage 11 embryos injected at one or two cell stage with Control or FAK morpholino (MO), β-actin was used as a loading control. (B) Quantification of FAK protein levels in stage 11 embryos, normalized to β-actin and shown relative to control embryos ($N=10$). Data are mean ± SEM. (C–F) Time matched views of representative Control and FAK MO injected embryos. (C) Vegetal view at mid gastrula (stage 11.5, arrowheads indicate blastopore lip, red arrowhead = dorsal). (D) Dorso-anterior view at late neurula (stage 22, red dashed line marks open neural tube). (E) Dorso-lateral view at early tailbud (stage 25). (F) Lateral view at late tailbud (stage 32). Stages given for control embryos, a = anterior, p = posterior. (G) Representative images and quantification of gastrulation phenotype (blastopore closure) in stage 12 Control and FAK MO injected embryos compared with embryos co-injected with FAK MO and cFAK ($N=7$, Control MO $n=371$, FAK MO $n=513$, FAK MO + cFAK RNA $n=327$). Embryos were counted as having defects if their development was more than 1 h behind that of control embryos, if there was failure to form or close the blastopore, or if the embryos died during gastrulation. The example given for "FAK MO + cFAK" was counted as rescued (a mild phenotype and not included in count of embryos with defects). (H) Representative images and quantification of tailbud phenotype (axial elongation and formation of anterior structures) in stage 33 Control and FAK MO injected embryos compared with embryos co-injected with FAK MO and cFAK ($N=4$, Control MO $n=225$, FAK MO $n=183$, FAK MO + cFAK RNA $n=217$). Embryos were counted as having defects if they failed to form eye anlagen, had a distinctly shortened anterior–posterior axis or failed to close the neural tube. The example given for "FAK MO + cFAK" was counted as rescued (a mild phenotype and not included in count of embryos with defects). Data in G and H are mean ± SEM. 25 ng MO injected per embryo. (I) Representative images from animal cap extension assay. Animal caps dissected from Control and FAK MO injected embryos with (+) and without (−) activin treatment ($N=4$, $n=40$/condition). (J) Representative images from Keller sandwich assay. Keller sandwiches made from Control and FAK MO injected embryos ($N=3$, $n=15$/condition). 20–25 ng MO and/or 200 pg RNA transcript injected per embryo.

(Fisher Scientific), 15 μmol/ml acrylic acid NHS ester (Fisher Scientific), 50 μM HEPES (4-(2-hydroxyethyl)-1-piperazineethanesulfonic acid; Fisher Scientific) was made and the pH of the solution adjusted to 5.9–6 with 1 M HCL. 50 μL of 1 μm-diameter fluorescent beads (Sphero carboxyl fluorescent particles; yellow; 1% w/v; Spherotech Inc., Lake Forest, IL) were added to 250 μL of the acrylamide solution, ammonium persulfate was added to initiate polymerization and the solution immediately cast onto cover slips pretreated with 3-aminopropyltrimethoxysilane and glutaraldehyde. The elastic modulus of the gel was directly measured (18.4 ± 1.9 kPa) by the ball indentation method (Dimitriadis et al., 2002). 30 μg of Fn (1 mg/mL) was diluted in 100 μL of 1 × MBS and added to each gel (26.5 μg Fn per cm^2 of gel). Mesendoerm explants were placed on top of the Fn coated polyacrylamide gel and allowed to adhere for 1 h. Time-lapse images of migrating explants and fluorescent beads were obtained between 1 h and 3 h after plating. Explants were trypsinized at the end of the imaging period to establish bead positions in the absence of traction forces. Gel deformations were calculated by quantifying bead displacements using a Particle Image Velocimetry (PIV) ImageJ plugin (Tseng et al., 2012). Traction forces were subsequently calculated utilizing Fourier transform traction cytometry (FTTC) (Butler et al., 2002), and average traction stresses were calculated by dividing the sum of all stress values at the leading edge by the number of points where traction stresses were calculated.

Western blots and co-immunoprecipitation

For Western blotting, 10 embryos per condition were solubilized in 200 μL lysis buffer: 100 mM NaCl, 50 mM Tris–HCl pH 7.5, 1% NP-40, 2 mM PMSF (phenylmethylsulphonylfluoride), and protease inhibitor cocktail (Sigma P2714). Phosphatase inhibitors were added as needed for pTyr (1 mM sodium orthovanadate and 0.2 mM H_2O_2) or pSer/Thr (1 mM EDTA, 1 mM EGTA, 1 mM β-glycerophosphate, and 2.5 mM $Na_4P_2O_7$). Yolk was removed by spinning samples for 5 min at 3000 rcf at 4 °C and moving supernatant (sample) to new tube. Protein extracts were diluted in 2 × reducing Laemmli buffer (5% β-mercaptoethanol), separated by SDS-PAGE (8 or 10%) then blotted onto nitrocellulose. Blots were probed with antibodies directed against FAK (2A7; Upstate, 05-182, used 1:500) (4.47; Millipore, 05-537, used 1:1000), Fn (4H2; Ramos et al., 1996, used 1:333), $pFAK^{Y397}$ (Life Technologies, 44624G, used 1:1000), $pFAK^{Y861}$ (Life Technologies, 44626G, used 1:1000), pMLC (Sigma, M6068, used 1:1000) or β-actin (Sigma, A3854, used 1:25,000) followed by appropriate HRP-conjugated secondary antibodies and ECL detection. For co-immunoprecipitation, 10 embryos per condition were solubilized in 100 μL lysis buffer: 100 mM NaCl, 50 mM Tris–HCl pH 7.5, 1% Triton X-100, 2 mM PMSF, 1 mM EDTA, 1 mM EGTA, 1 mM β-glycerophosphate, 2.5 mM $Na_4P_2O_7$, 1 mM sodium orthovanadate and 0.2 mM H_2O_2. Yolk was removed as described above and 1 embryo equivalent was used for western blot and the remaining sample brought up to 500 μL in lysis buffer. Target proteins were immunoprecipitated overnight at 4 °C using 50 μL protein-G agarose beads per sample (Roche) that were pre-incubated with antibodies against plakoglobin (BD Biosciences, 610253, 4 μg/500 μL) or β-catenin (Sigma, C2206, 4 μg/500 μL) at 4 °C for 1 h. The precipitates were diluted in 2 × reducing Laemmli buffer and separated by SDS-PAGE (8%) then immunoblotted with an antibody against C-cadherin (6B6, supernatant used 1:6 in TBST; Brieher and Gumbiner, 1994; courtesy of Barry Gumbiner).

Statistical analyses

Assembly of data and statistical analyses were performed with Microsoft Excel and PAST (http://folk.uio.no/ohammer/past; Hammer et al., 2001). For pairwise comparisons in which the data were consistent with a Gaussian distribution (as determined by the Shapiro–Wilk test), an *F*-test was used to check for equal variance followed by either a *t*-test or an unequal variance *t*-test. Non-parametric tests were used for datasets in which an assumption of Gaussian distribution was not valid. Levene's test was used to test for equal variance, followed by either a Mann–Whitney test (for datasets consistent with an assumption of equal variance) or a Kolmogorov–Smirnov test (for datasets with unequal variance). Circular statistics were used for analyses of protrusion direction, either Rayleigh's test for randomness of distribution or the Mardia–Watson–Wheeler test for the comparison of two sample groups. Correlation analyses were performed using Kendall's tau test. In each case where multiple analyses of the same data were performed, the Holm–Bonferroni correction was applied to ensure that the type I error rate was not inflated; this did not affect the significance of any comparisons.

Results

FAK is required for normal blastopore closure and axial elongation

We designed an antisense morpholino oligodeoxynucleotide (MO) to block translation of *Xenopus* FAK mRNA in order to investigate the functions of FAK in early morphogenetic movements. Although previous studies using different sets of morpholinos targeted to FAK reported no effects on gastrulation (Doherty et al., 2010; Fonar et al., 2011), those sequences were shown to knock down FAK expression by only 30–50% at gastrulation (Doherty et al., 2010; Petridou et al., 2012). Injection of the FAK MO selected for this study effectively inhibited translation of co-injected xFAK transcript (Fig. S1A) and resulted in > 70% reduction in endogenous FAK protein expression by gastrula stages (Fig. 1A, B). Remnant FAK expression in gastrula stage morphant embryos was equivalent to the level of protein present at 1-cell stage (Fig. S1B), suggesting that the FAK remaining in morphant gastrulae is due to the persistence of maternal FAK protein translated during oogenesis.

In FAK morphant embryos, the appearance of the dorsal blastopore lip was delayed by about 90 min relative to age matched control embryos (data not shown). Closure of the blastopore (Fig. 1C, arrowheads) was also delayed in FAK morphant embryos. Significant lethality was evident during gastrulation with approximately 60% of embryos surviving to tailbud stages. The majority of surviving embryos failed to form normal anterior structures including eye anlagen, otic vesicles, and pharyngeal grooves. Other embryos failed to close portions of the neural tube, particularly at the anterior end (Fig. 1D; Fig. S2A, B). Onset of axial elongation was delayed in FAK morphant embryos (Fig. 1D, E) and morphants remained truncated along the anterior–posterior axis, relative to controls, with a pronounced curve toward the dorsal aspect (Fig. 1F). Additional tailbud stage defects included disorganization of the neural tube, the presence of cells within the neurocoel, lack of vacuolation of cells in the notochord, failure to extend the notochord to the posterior of the embryo, and malformed gut epithelia (Fig. S2C–D′). We also noted failures in the alignment and elongation of somites in FAK morphants (Fig. S2E, F). None of the FAK morphant embryos survived to tadpole stages. Control embryos were indistinguishable from uninjected embryos throughout development (data not shown). FAK protein levels (Fig. S1C) and the gross morphological phenotypes of FAK morphants (Fig. 1G, H) were partially rescued by co-expression of the chicken ortholog of FAK (cFAK). The sequence of cFAK is sufficiently dissimilar to that of xFAK in the region targeted by the MO that its translation is not inhibited by FAK MO. These

rescue experiments indicate that the observed phenotypes are due to the specific knockdown of FAK.

Animal cap extension assays were performed to further investigate the defect in axial elongation. When animal cap ectoderm is dissected from control embryos at stage 8, it forms a ball of cells that elongates in response to treatment with the mesoderm inducing factor activin (Symes and Smith, 1987) and has thus been used as a model of convergence and extension movements (e.g. Ninomiya et al., 2004). Animal caps obtained from FAK morphant embryos did not respond to activin treatment by extending, rather they remained globular and formed multiple small protuberances (Fig. 1I). To confirm this finding, mesoderm explants (Keller sandwiches) were prepared from control and FAK morphant embryos (Keller and Danilchik, 1988). Extension of Keller sandwiches prepared with FAK morphant mesoderm tissue was reduced relative to that of controls (Fig. 1J). Thus, extension of the anterior–posterior axis was disrupted in whole embryos, activin-induced animal caps and isolated mesoderm tissues. Moreover, elongation of intact embryos was partially rescued by co-injection of cFAK RNA with FAK MO. Together, these data indicate that normal FAK expression is required for axial elongation movements.

Phenotypes of FAK morphant embryos were similar to those of Fn morphants (Davidson et al., 2006) which in turn resemble embryos unable to deposit FN matrix following injection of function blocking antibodies (Marsden and DeSimone, 2003). However, Fn protein levels and assembly of Fn matrix on the blastocoel roof appeared normal in FAK morphant embryos (Fig. S3A–C). A previous study found that pFAK^{Y397} is highly enriched in the animal cap cells that assemble the Fn matrix (Petridou et al., 2012). Phosphorylation of FAK at the auto-phosphorylation site Tyr397 is commonly used as a readout for FAK kinase activity (Schlaepfer et al., 1999). Interestingly, we found that the FAK protein that remains in FAK morphant embryos was phosphorylated on Tyr397 at only slightly lower levels than non-morphant controls (Fig. S3D). In contrast, FAK phosphorylated by Src at Tyr861 is normally enriched in mesoderm and mesendoderm (Petridou et al., 2012) and was greatly attenuated in FAK morphant embryos (Fig. S3E). These data suggest that the residual level of pFAK^{Y397} in morphant embryos (Fig. S3D) is sufficient to support assembly of Fn matrix along the blastocoel roof (Fig. S3B) where pFAK^{Y397} is normally enriched (Petridou et al., 2012). Therefore, it is unlikely that the defects in gastrulation movements observed in FAK morphants are due to lack of Fn matrix assembly along the blastocoel roof.

Mesendoderm from FAK morphant embryos migrates more slowly and with less persistence

Bisection of fixed embryos at various time points throughout gastrulation was used to reveal the morphology and progression of mesendoderm tissue in vivo. In control embryos, mesendoderm migration begins with the formation of a ridge of tissue on the dorsal side of the embryo at the margin between involuting mesoderm and the endodermal mass (Fig. 2A, Control MO, red arrowhead). Ventral and lateral mesendoderm cells follow suit, forming a ring or cup of tissue moving cohesively toward the animal pole (Davidson et al., 2002). In contrast, formation of the dorsal mesendoderm ridge was delayed in FAK morphants, with both dorsal and ventral tissue simultaneously initiating translocation across the blastocoel roof (Fig. 2A, FAK MO, red arrowheads). The progression of the mesendoderm tissue toward the animal pole of FAK morphant embryos lagged behind that of Control MO injected embryos by 1.5–2 h and the leading edge of the tissue was uneven. The appearance and elongation of Brachet's cleft (Fig. 2A, arrow, Bc) was delayed in FAK morphants, consistent with a delay in advancement of the mesendoderm tissue. Thinning of the marginal tissue was also disrupted in FAK morphants (Fig. 2A, brackets in middle panels) but there was no effect on radial intercalation in the blastocoel roof (Fig. 2A, arrow, bcr), which appeared to thin normally.

To better observe the behavior of cells within the mesendoderm we utilized explants comprised of tissue excised from the dorsal marginal region of the embryo. These explants were placed in a simple salt solution (i.e. MBS) on Fn coated coverslips or Fn coated PDMS gels. Mesendoderm explants are commonly used to recapitulate “ex vivo” the organization and behavior of mesendoderm tissue as it would normally occur in the intact embryo (Davidson et al., 2004, 2002). We found that the average velocity (displacement/time) of mesendoderm cells in the leading rows of explants taken from FAK morphant embryos was reduced on both glass and the softer gel substrate, resulting in a decreased rate of tissue advancement relative to controls (Fig. 2B). Similarly, single mesendoderm cells from dissociated FAK morphant tissue had a lower average velocity than control cells. Both single cells and explanted tissues from FAK morphant embryos moved less persistently than controls (Fig. 2C). Single mesendoderm cells from control embryos moved in apparently random directions with low persistence, calculated as displacement divided by path length. Cells in explants from control embryos migrated collectively and with a high degree of directionality and persistence. However, no significant increase in persistence of cells was observed in tissue explanted from FAK morphant embryos compared with single FAK morphant cells. Both velocity and persistence of migration of FAK morphant cells in mesendoderm explants were rescued by co-injection of cFAK RNA, which is not targeted by the FAK MO (Fig. 2D, E). These data indicate that FAK is required for persistent migration of mesendoderm cells and, in contrast to control cells, the influence of neighboring cells is not sufficient for establishment of persistent migration. The meandering behavior exhibited by FAK morphant cells likely contributes to the decreased rate of mesendoderm tissue advancement observed in explants and intact embryos.

FAK contributes to regulation of protrusion number and protrusive polarity

We analyzed protrusive activity in mesendoderm explants expressing membrane localized GFP in order to determine whether the meandering behavior of FAK morphant cells reflects changes in directional polarity during collective migration. Yolk free extensions from the cell body were designated as protrusions and the directions and total numbers of these protrusions were measured for cells in the first four rows of the migrating explants. Retracting edges, identified by time-lapse imaging, and fine filopodia-like extensions were excluded from the quantification. Most cells within control explants displayed monopolar protrusive behavior, extending one or two lamellipodial protrusions toward the contiguous leading edge of the migrating tissue (Fig. 3A). Cells in tissue explanted from FAK morphant embryos frequently extended protrusions in directions other than the expected direction of tissue migration, in addition to protrusions in the expected direction (Fig. 3B). Uneven progression of the leading edge was also evident in FAK morphant explants. Quantification of protrusion number in explants revealed that control cells extended an average of 1.71 protrusions per cell while FAK morphant cells had a significantly higher average of 1.96 protrusions per cell (Fig. 3C). To determine directionality of protrusions, the angle of each protrusion was measured relative to a line running through the cell centroid and parallel to the direction of migration. The predicted direction of tissue advancement was defined as 180°. Angles from the entire population of control or FAK morphant cells were binned into twelve 30° increments and the percent of angles in each bin calculated. As previously reported (Weber et al., 2012), cells in control explants extend the majority of their protrusions toward 180° ($\pm$15°) with no protrusions extended greater than 90° away from the direction of

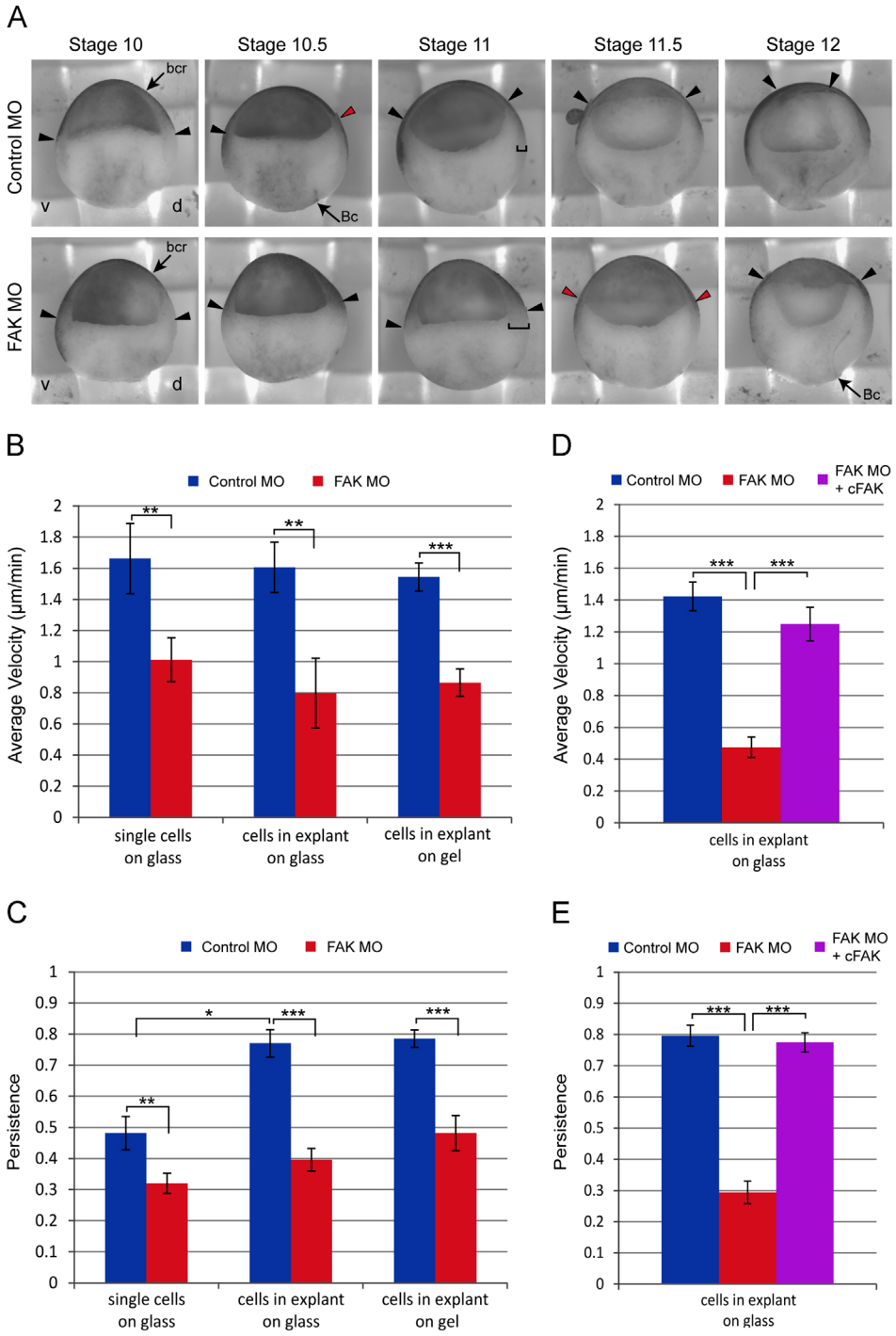

Fig. 2. FAK morphant mesendoderm cells migrate slowly and lack persistence. (A) Sagittal views of representative Control or FAK MO injected embryos from the same clutch that were fixed and bisected at time matched stages from early gastrulation (stage 10) through late gastrulation (stage 12). Arrowheads indicate position of the mesendoderm mantle, red arrowheads mark the first displacement between the mesendoderm and the blastocoel roof (bcr), red brackets mark the thickness of the marginal tissue, Bc=Brachet's cleft, *d*=dorsal, *v*=ventral. (B, C) Quantification of average velocity (B, displacement/time) and persistence (C, displacement/path length) of single mesendoderm cells on glass ($N=3$, Control MO $n=32$, FAK MO $n=65$), cells in mesendoderm explants on glass ($N=3$, Control MO $n=19$, FAK MO $n=23$), and cells in mesendoderm explants on gels ($N=3$, Control MO $n=22$, FAK MO $n=20$). (D, E) Quantification of rescue of average velocity (D, displacement/time) and persistence (E, displacement/path length) of cells in mesendoderm explants on glass by co-injection of FAK MO with cFAK RNA ($N=3$, Control MO $n=30$, FAK MO $n=32$, FAK MO+cFAK RNA $n=30$). Data are mean ± SEM. $^{*}p<0.05$, $^{**}p<0.01$, $^{***}p<0.001$. 20–25 ng MO and/or 200 pg RNA transcript injected per embryo.

tissue migration (Fig. 3D, expected direction indicated in green). The directional distribution of protrusions in FAK morphant explants was significantly broadened, with a small but significant number of protrusions extended at angles more than 90° from the expected direction of migration (Fig. 3D, aberrant directions indicated in yellow and red).

Additional analyses of protrusive behavior were performed by grouping cells according to distribution of their protrusions. In FAK morphant explants, we observed a significant decrease in the percent of cells only extending protrusions within 45° of the expected direction of tissue migration (set as 180°) (Fig. 3E). 9% of FAK morphant cells extended protrusions only in the direction

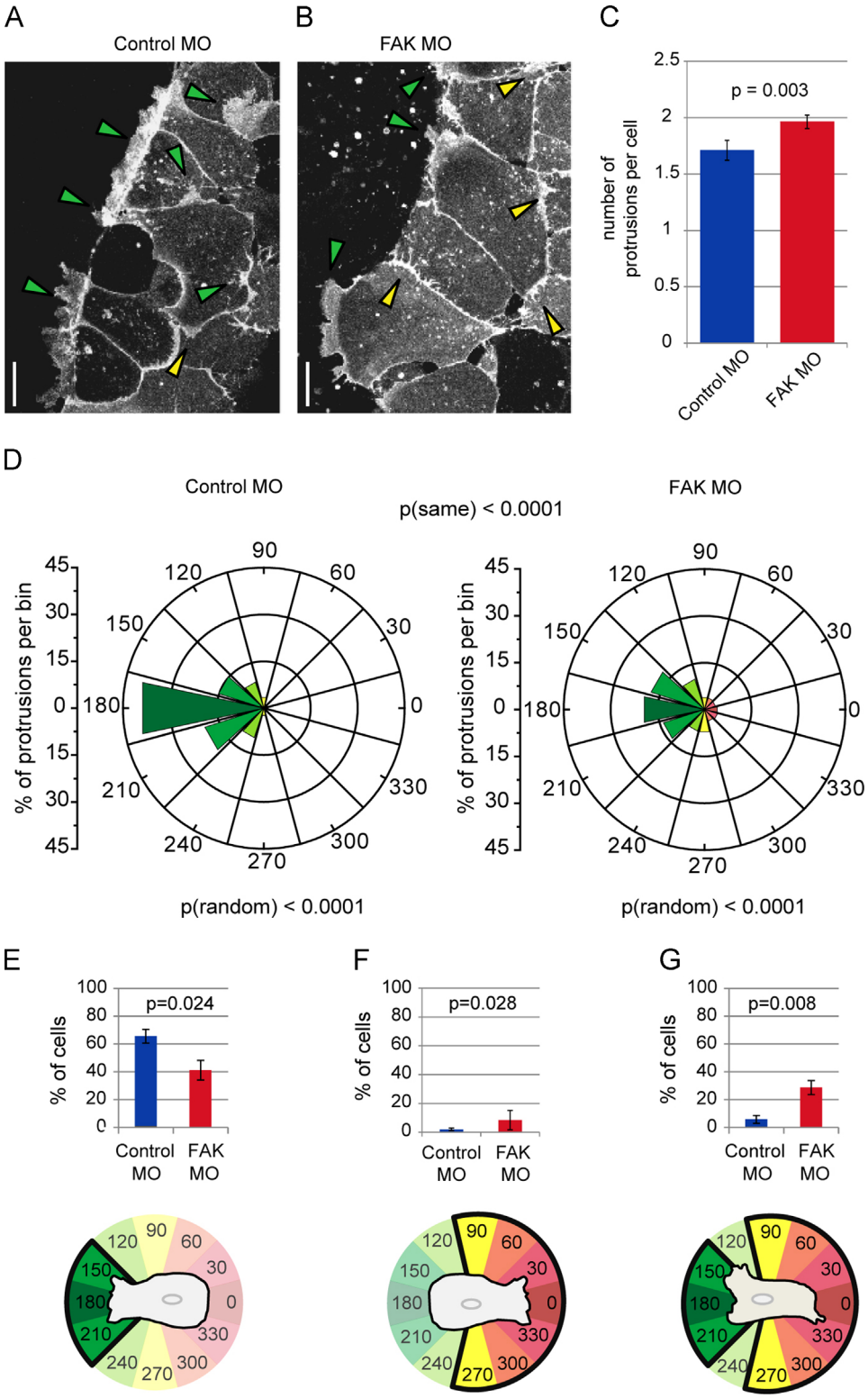

Fig. 3. FAK is essential for normal polarity of migrating mesendoderm. (A and B) Representative collapsed 5 μm z-stack images of live cells in control (A) and FAK morphant (B) mesendoderm explants expressing GAP-43-GFP to label membranes. Green arrowheads highlight protrusions in the expected direction of tissue movement and yellow arrowheads mark protrusions in any other direction. (C) Quantification of protrusions per cell in control and FAK morphant mesendoderm explants. Data are mean ± SEM. (D) Quantification of protrusion angles of mesendoderm cells in explants from control ($N=4$, $n=100$) and FAK morphant ($N=4$, $n=210$) embryos, relative to cell centroids (center of rose diagram). 180° is defined as the predicted direction of normal tissue movement and marked in dark green. Mis-directed protrusions at 90° or 270° are marked in yellow and those at 0° are marked in red. *Y* axis for the rose diagrams represents percent of protrusions in each directional bin. Protrusions were quantified in both leading (row 1) and following (rows 2–4) cells. Significance was evaluated using circular statistical tests for randomness of distribution (Rayleigh's test, p(random)) and similarity of distribution (Mardia–Watson–Wheeler, p(same)). (E–G) Additional quantification of the data set shown in (D), indicating the percent of control or FAK morphant cells in mesendoderm explants with protrusions in the area defined in the cartoon beneath each graph, color coded to match graphs in (C). Data are mean ± SEM. (E) Percent of cells with protrusions only within 45° of the direction of tissue migration. (F) Percent of cells with only protrusions deviating 75° or more from the direction of travel. (G) Percent of cells with at least one protrusion in the direction of travel and also one or more greater than 75° away from the expected direction of tissue migration. Scale bars=25 μm. 20–25 ng MO injected per embryo.

opposite the leading edge, quantified as any direction greater than 75° off axis (105–255°) (Fig. 3F). This is in contrast to control cells that did not extend any protrusions toward the rear of the explant, with only two protrusions near 90° (out of a total of 100 counted protrusions). 29% of cells in FAK morphant explants had off-axis protrusions (105–255°) in addition to at least one protrusion in the predicted direction (225–135°), a significant difference from the protrusive behavior observed in control cells (Fig. 3G). Taken together with the increase in number of protrusions per cell, these data suggest that FAK is important for limiting off-axis protrusions from mesendoderm cells in the intact tissue.

Actin organization is altered in FAK morphants

While quantifying the number and polarity of protrusions extended by FAK morphant mesendoderm cells we noted a marked difference in the morphology of these protrusions. In FAK morphant explants, an abundance of filopodia-like extensions were evident in addition to a significant increase in the average number of lamellipodial protrusions per cell. Because actin organization is integral to protrusion morphology, we investigated whether changes in protrusions were accompanied by changes in actin organization. Expression of a GFP tagged version of the actin binding protein moesin was used to visualize the actin filament network in control and FAK morphant cells. Cells in control explants extended broad lamellipodial protrusions across the leading edge with smaller lamellipodial extensions in the cells in following rows (Fig. 4A, green arrowheads). These lamellipodia were filled with a dense meshwork of actin amongst fine bundles of filaments. While broad lamellipodia were occasionally observed in FAK morphant explants, these cells typically had narrower and more dynamic protrusions which contained actin spikes and generally lacked the dense actin network present in protrusions of control cells (Fig. 4B, yellow arrowheads). This finding suggests that FAK is important for the organization of the lamellipodia, or perhaps the dynamics of the actin network in protrusions.

Actin filaments in the body of control cells were typically distributed around the cell cortex and organized in a fine mesh throughout the cytoplasm, with slight enrichment at the midpoint or rear of some cells (Fig. 4C, green arrowheads). A cortical distribution of actin filaments was observed in the body of most cells in FAK morphant explants; however, there was an increased prevalence of stress fibers spanning the cells (Fig. 4D, yellow arrowheads). In contrast with control cells (Fig. 4E), FAK morphant cells were also frequently observed to have numerous filopodia-like protrusions along their lateral edges where they contact neighboring cells, perhaps indicative of changes in cell–

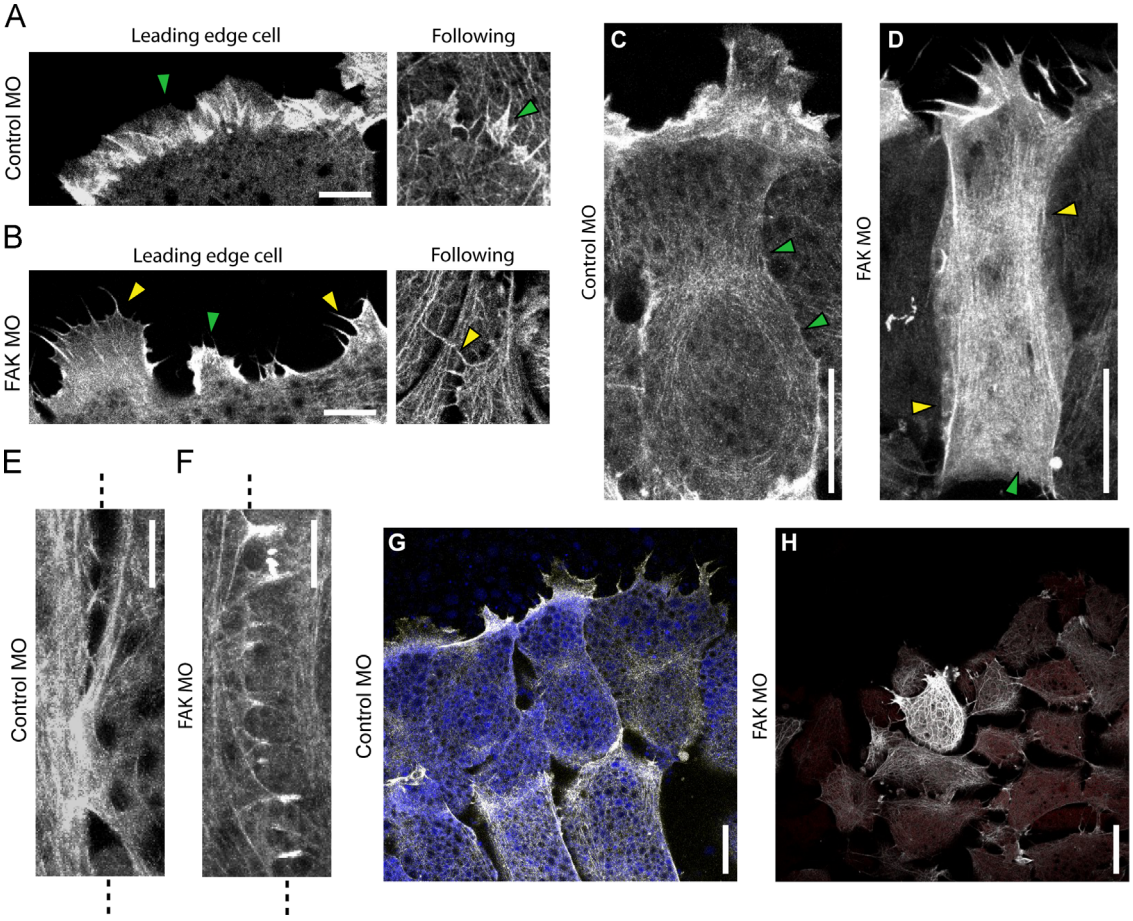

Fig. 4. Actin organization is altered in FAK morphant cells. (A–E) Representative confocal images of live cells in mesendoderm explants expressing GFP–moesin to label the actin filament network. (A) Single plane confocal images of actin at the leading edges of cells in the first row (left) and following rows (right) of control mesendoderm explants. Green arrowheads indicate actin rich protrusions. (B) Single plane confocal images of actin on the leading edges of cells in the first row (left) and following rows (right) of FAK morphant mesendoderm explants. Yellow arrowheads indicate actin microspikes. (C) Collapsed 7.5 μm z-stack image of actin in a cell on the leading edge cell of a control explant. Greed arrowheads indicate cortical actin. (D) Collapsed 7.5 μm z-stack image of actin in a cell on the leading edge of a FAK morphant explant. Green arrowhead indicates cortical actin; yellow arrowheads indicate actin stress fibers. (E, F) Collapsed 5.5 μm z-stack images of cell–cell junctions in following rows of control (E) and FAK morphant (F) explants. Dashed lines mark the boundary between cells. (G) First frame from time-lapse confocal imaging of live cells in control mesendoderm explants (See Movie 1). Collapsed 5 μm z-stack image. Cells also labeled with fluorescently tagged dextran (blue) to show cell shape. (H) First frame from time-lapse confocal imaging of live cells in FAK morphant mesendoderm explants (See Movie 2). Collapsed 5 μm z-stack image. Cells also labeled with fluorescently tagged dextran (red) to show cell shape. Scale bars = 10 μm (A, B, E) or 25 μm (C, D, G, H). 20–25 ng MO injected per embryo.

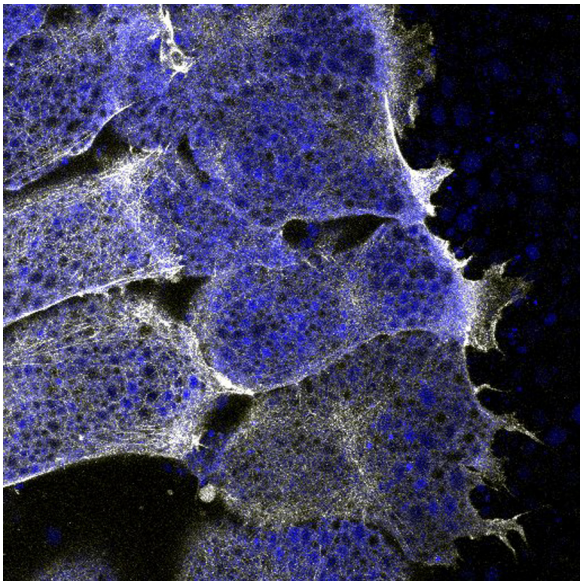

Movie S1. Normal migration, morphology and protrusion dynamics in migrating mesendoderm. Time-lapse confocal images of live cells in Control MO injected mesendoderm explants (25 ng MO per embryo) expressing GFP–moesin (500 pg transcript per embryo) to label the actin filament network. Cells also labeled with fluorescently tagged dextran (blue) to show cell shape. Each frame is a collapsed 5 μm z-stack image. One frame was collected every 30 s for 10 min. Playback rate is 6 frames per second. A video clip is available online. Supplementary material related to this article can be found online at http://dx.doi.org/10.1016/j.ydbio.2014.07.023.

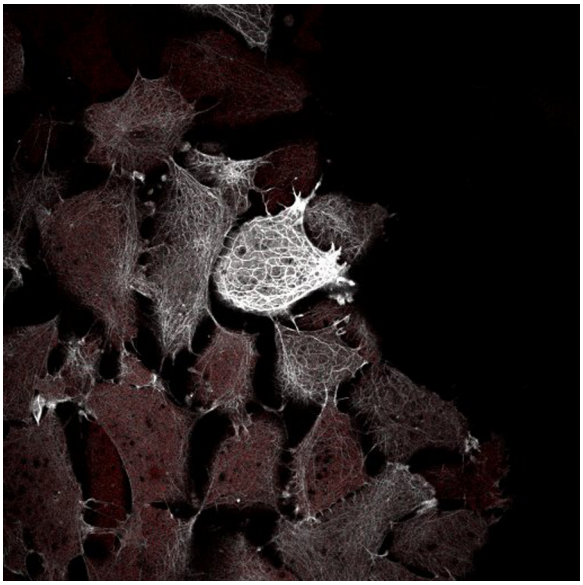

Movie S2. FAK morphant mesendoderm cells are less spread, migrate more slowly and extend smaller, less persistent protrusions. Time-lapse confocal images of live cells in FAK MO injected mesendoderm explants (25 ng MO per embryo) expressing GFP–moesin (500 pg transcript per embryo) to label the actin filament network. Cells also labeled with fluorescently tagged dextran (red) to show cell shape. Each frame is a collapsed 5 μm z-stack image. One frame was collected every 30 s for 10 min. Playback rate is 6 frames per second. A video clip is available online. Supplementary material related to this article can be found online at http://dx.doi.org/10.1016/j.ydbio.2014.07.023.

cell adhesion (Fig. 4F). Although actin organization was abnormal in FAK morphant cells no change was detected in phosphorylation of myosin light chain, suggesting that acto-myosin contractility was unaltered (Fig. S5A, B). In summary, actin organization in the cell bodies and protrusions of cells in FAK morphant explants differed significantly from controls (Fig. 4G, H and Movies 1 and 2). FAK morphant cells retained the ability to extend protrusions and form cell–cell junctions, albeit in abnormal forms in both cases.

FAK is required for organization of the keratin filament network

Expression and organization of keratin is integral to protrusive polarity in collectively migrating mesendoderm cells (Weber et al., 2012). Because cell polarity was disrupted in FAK morphant mesendoderm tissue we investigated whether keratin organization might also be disrupted in these cells. Expression of GFP labeled keratin (GFP-XCK1 (8)) was used to visualize the organization of the keratin filament network in live FAK morphant explants. In control tissues, keratin filaments are typically most prominent at the rear of each cell where they often form a basket-like arrangement (Fig. 5A, green arrowheads). In embryos and in mature mesendoderm explants (those that have been migrating for 1 h or more), keratin filaments also form a cable along leading edge cells, just behind and dorsal to the lamellipodia as well as between cells (Fig. 5B, green arrows). This organization was severely disrupted in explants from FAK morphant embryos; filaments were distributed throughout each cell and often biased toward the front of leading edge cells (Fig. 5C, yellow arrowheads). Furthermore, the cable-like connections behind the lamellipodia and between cells were absent under these conditions (Fig. 5D, yellow arrows). The degree of disrupted filament organization in each cell appeared to be correlated with alterations in cell spreading and polarity. In well-spread cells with forward facing lamellipodia we observed rearward, basket-like localization of keratin filaments, while in less well polarized cells we observed random localization or an increase in filaments at the cell front. Many cells with round morphology were evident in FAK morphant explants (Fig. 5D, dashed yellow line). The keratin filaments in these cells were organized in a wagon-wheel arrangement similar to that observed in pairs of cells plated on poly-L-lysine substrates that do not support generation of traction forces (Weber et al., 2012). Both the rearward localization and cabling of keratin filaments were rescued by co-expression of cFAK (Fig. 5E, F, green arrowheads and arrows). These findings indicate that FAK is essential for organization of the keratin filament network in collectively migrating mesendoderm cells.

Spreading and cell traction on Fn is reduced in FAK morphants

FAK morphant cells in intact explants appeared less well spread and less adherent to Fn than cells in control explants. Furthermore, the wagon-wheel arrangement of keratin filaments observed both in cells in FAK morphant explants (Fig. 5D) and in cell groups on poly-L-lysine (Weber et al., 2012) suggested that generation of traction force on the substrate might be affected by loss of FAK. To quantify the effects of diminished FAK expression on cell spreading we plated isolated mesendoderm cells from both control and FAK morphant embryos on Fn coated coverglass (Fig. 6A) and tallied the percent of cells spread (Fig. 6B). FAK morphant mesendoderm cells attached to the substrate but were about 30% less likely to be fully spread.

We then measured traction forces generated by individual control and FAK morphant mesendoderm cells isolated from the leading edge of the mesendoderm and plated on Fn coated arrays of deformable microposts (Yang et al., 2011). FAK morphant cells generated significantly less total traction force per cell (sum of forces applied to all posts under each cell) (Fig. 6C), but there was no significant change in the average force per post (Fig. S5A). Thus, there is less total traction being applied by FAK morphant cells because they have proportionally less contact with the substrate. Calculation of the circularity of control and FAK morphant cells

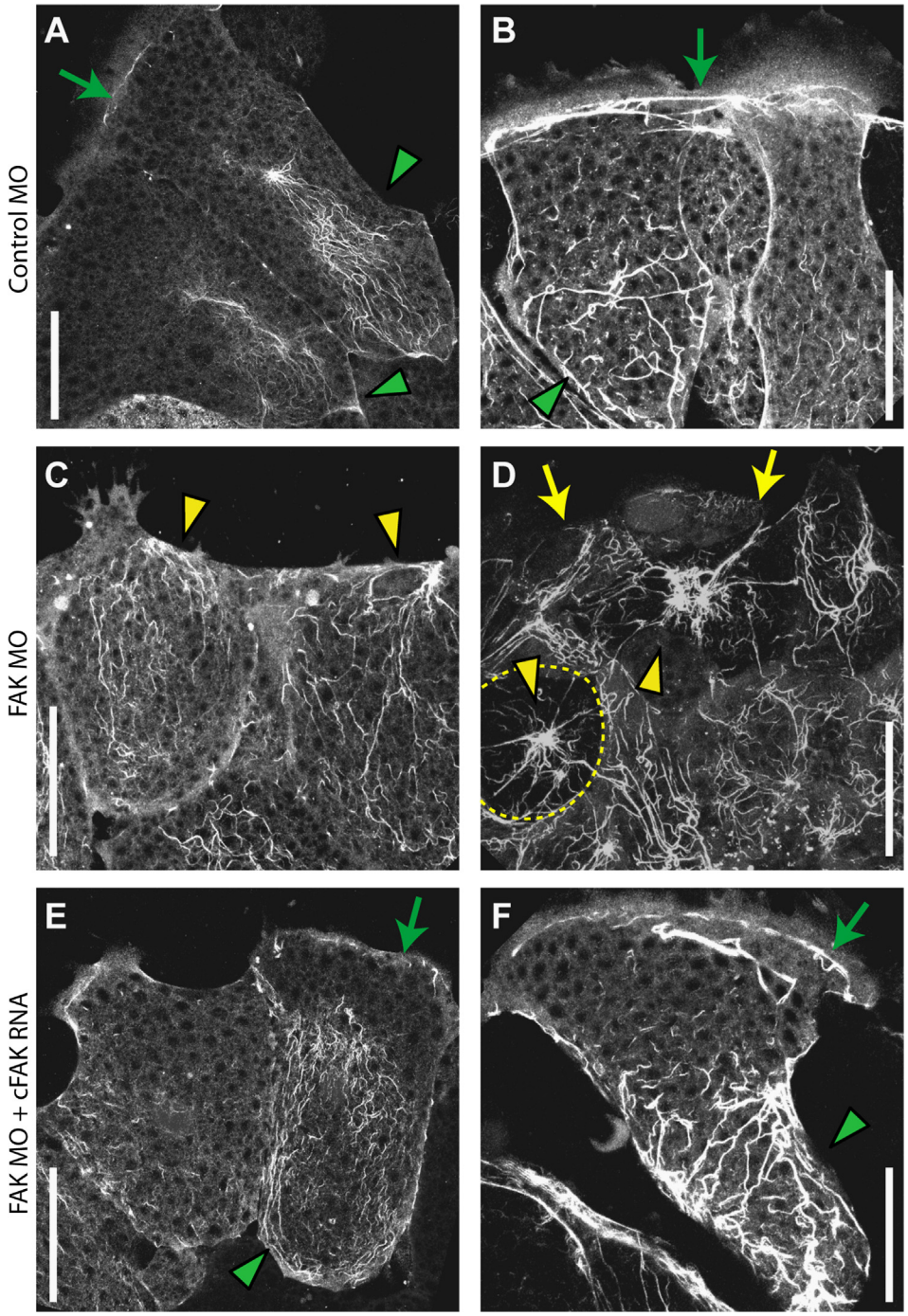

Fig. 5. FAK is required for organization of the keratin filament network. (A–F) Representative collapsed 10 μm z-stack images of live cells in mesendoderm explants expressing GFP-XCK1 (8) to label the keratin filament network. (A, B) Keratin filaments in leading edge cells in control explants. Green arrowheads indicate basket like arrangement of filaments in the rear of each cell, green arrows indicatecabling across the leading edge cells. (C, D) Keratin filaments in leading edge cells in FAK morphant explants. Yellow arrowheads indicate mis-localized filaments, yellow arrows indicate loss of cabling, yellow dashed line in (D) denotes cell outline. (E, F) Keratin filaments in leading edge cells in explants co-injected with FAK MO and cFAK RNA, which is not targeted by the morpholino. Green arrowheads indicate basket-like arrangement of filaments, green arrows indicate cabling across leading edge cells. Scale bars=50 μm. 20–25 ng MO injected per embryo.

using the same images as those from which traction data were gleaned revealed a significant increase in roundness in FAK morphant cells, indicating a decrease in the degree of spreading (Fig. 6D, E). Indeed, the two measures were strongly correlated; well-spread cells tended to exert more force on the Fn substrate than poorly-spread cells (Fig. S5B, C). There was a statistically significant correlation between circularity and total cell force for both control cells and FAK morphant cells (Control MO; $p=0.038$, FAK MO: $p=0.0009$). The average traction stresses generated at the leading edge of FAK morphant mesendoderm explants migrating collectively on deformable gels were also significantly decreased (Fig. 6F). We conclude that FAK is a critical component of the substrate traction machinery in mesendoderm cells, and disruption of FAK function leads to alterations in the mechanical properties and morphology of mesendoderm tissue.

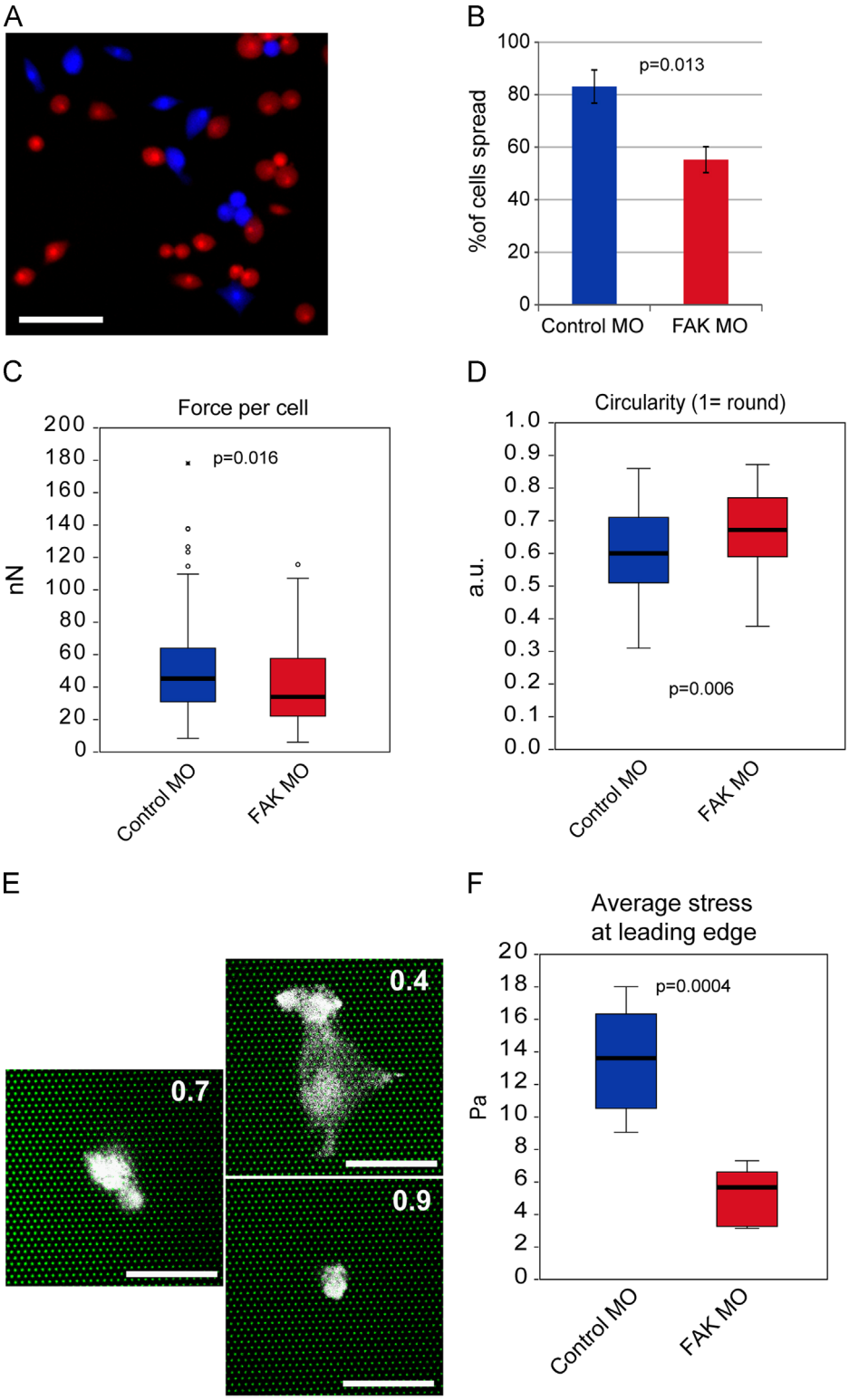

Fig. 6. Spreading and cell traction are reduced in FAK morphant mesendoderm cells. (A) Representative image of control (blue) and FAK morphant (red) mesendoderm cells plated on Fn coated coverglass. Cells labeled with fluorescently tagged dextran to show cell shape and mark control vs. FAK morphant cells. (B) Quantification of percent of mesendoderm cells spread on Fn coated coverglass ($N=3$, Control MO $n=88$, FAK MO $n=97$). Data are mean ± SEM. (C) Quantification of average force per cell exerted by mesendoderm cells on Fn coated micropost arrays ($N=4$, Control MO $n=74$, FAK MO $n=56$). (D) Quantification of circularity of cells from (C). (E) Examples of cells from (D) illustrating the circularity values indicated in top right corner of each panel. Cells labeled with fluorescently tagged dextran to show cell shape, microposts are shown in green. (F) Quantification of average stress applied by leading edge cells of mesendoderm explants to Fn coated polyacrylamide gels ($N=3$, $n=6$ explants/condition). Data in (C, D, F) are shown in box–whisker plots, bold line indicates mean, box delimits 25th–75th percentile and whiskers mark minimum and maximum values, statistical outliers are marked as dots. Scale bars=200 μm (A) or 50 μm (E). 25 ng MO injected per embryo.

FAK is important for association of plakoglobin with cadherin

Previous work in this system has demonstrated the importance of anisotropic tension in the recruitment of plakoglobin (also known as γ-catenin) and keratin to cell–cell contacts, and the importance of plakoglobin expression for polarity of protrusions in the migrating tissue (Weber et al., 2012). In light of these findings, and our observations of diminished traction and disrupted organization of keratin filaments in FAK morphant cells, we hypothesized that loss of FAK would have a negative effect on assembly of the plakoglobin-containing adhesion complex. We investigated the assembly of these complexes, specifically the linkage between C-cadherin (cdh3) and plakoglobin, by performing co-immunoprecipitation analyses. During early gastrulation (stage 10), when the mesendoderm is just beginning to migrate, there was a reduction in the association of plakoglobin with C-cadherin in FAK morphant embryos relative to controls (Fig. 7A, B). However, at the end of gastrulation (stage 12) there was no longer a significant difference noted in the association of plakoglobin with C-cadherin in FAK morphant embryos. Loss of FAK expression had no effect on the association of β-catenin with C-cadherin at either time point (Fig. 7A, C). These results are consistent with a role for FAK in regulation of the tension-dependent recruitment of plakoglobin to cell–cell junctions during the establishment of polarity in migrating mesendoderm.

Discussion

This study supports a critical role for FAK in the morphogenetic movements of early development including mesendoderm migration, neural tube closure and axial elongation. Furthermore, we show that FAK is required for normal subcellular organization of keratin intermediate filaments and for assembly of a cadherin–plakoglobin adhesion complex. Both of these events were reported previously to be dependent on cell–cell tension and essential for guidance of collective mesendoderm migration (Weber et al., 2012). The data presented here suggest that FAK is essential for development of tension in the mesendoderm and therefore acts upstream of keratin and plakoglobin to guide migratory polarity of the tissue in vivo.

FAK function in vertebrate development

A requirement for FAK in the normal development of mesodermal derivatives, such as the notochord and somites, is shared among several vertebrate species including mouse, zebrafish, and *Xenopus* (Crawford et al., 2003; Furuta et al., 1995; Henry et al., 2001; Hens and DeSimone, 1995; Kragtorp and Miller, 2006). We report here that FAK is also essential for gastrulation movements in *Xenopus*, particularly for the coordination of collective migration of mesendoderm. These findings confirm those of a study using the dominant negative FAK splice variant FRNK (Fak related non-kinase) in which blastopore closure and mesendoderm migration were slowed or disrupted (Stylianou and Skourides, 2009), although underlying cell behaviors were not previously reported. Evidence indicates that FAK also plays a critical role in closure of the neural tube and in axial elongation, but with some variations noted in the presence and degree of phenotypes resulting from different experimental perturbations. For example, injection with FAK MO (Fig. 1D and Fonar et al., 2011) or transcript encoding FRNK (Stylianou and Skourides, 2009) leads to defects in closure of the neural tube. However, injection of the dominant negative FAK construct FF, which lacks the kinase domain and is thought to act by displacing endogenous FAK, has no apparent effect on neural tube closure (Petridou et al., 2013). Interestingly, injection of FAK MO (Fig. 1F and

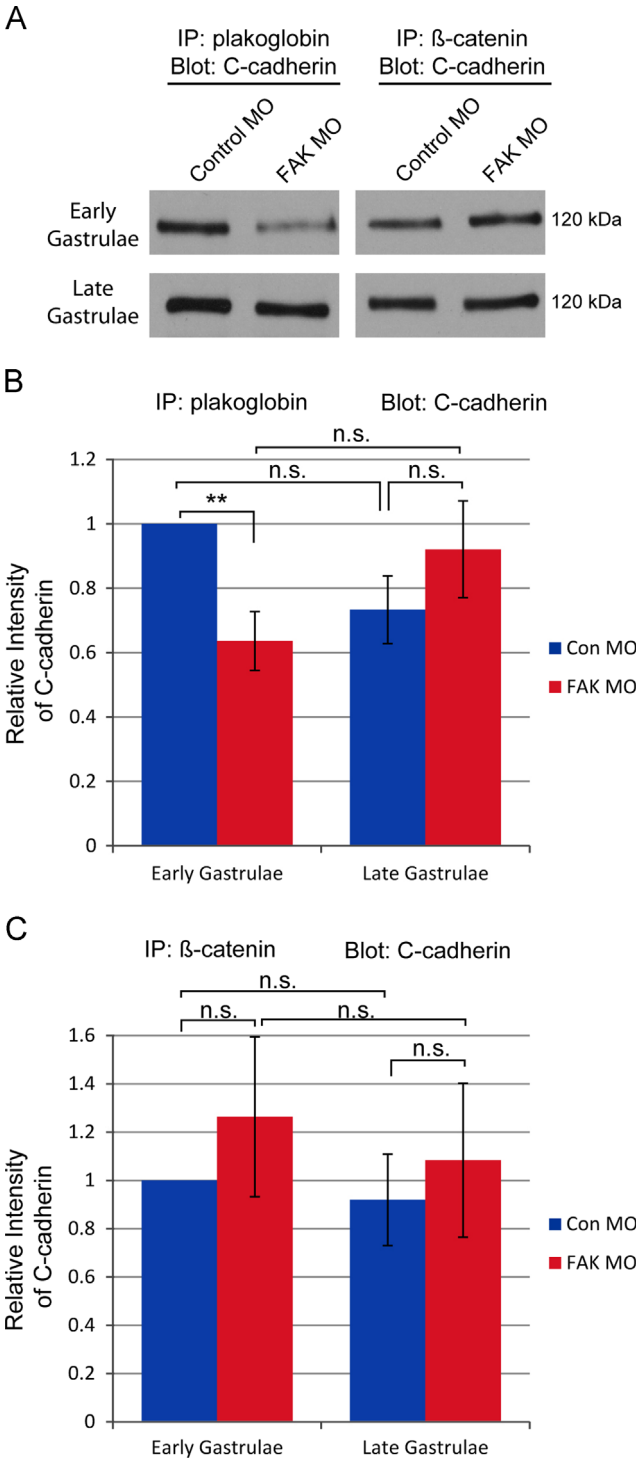

Fig. 7. Association of plakoglobin with C-cadherin is disrupted in early FAK morphant gastrulae. (A) Representative Western blot of plakoglobin or β-catenin immunoprecipitates from whole embryo lysates of control or FAK morphant embryos, probed with an antibody directed against C-cadherin. (B) Quantification of C-cadherin association with plakoglobin in early (stage 10) and late (stage 12) gastrulae injected with Control or FAK MOs. (C) Quantification of C-cadherin association with β-catenin in early (stage 10) and late (stage 12) gastrulae injected with Control or FAK MOs. Embryos from the same clutch were used for both plakoglobin and β-catenin co-immunoprecipitation at early and late stages of gastrulation ($N=3$). Blots were re-probed with antibodies directed against plakoglobin or β-catenin respectively and scans of these blots were used to normalize scans of C-cadherin blots, all values are shown relative to early control gastrulae. Data are mean ± SEM. $^{**}p=0.003$. 25 ng MO injected per embryo.

Fonar et al., 2011) or expression of FF (Petridou et al., 2013) severely disrupt axial elongation, but FRNK expression has no notable effect on embryo length (Stylianou and Skourides, 2009). Despite some

differences, these data together indicate that normal zygotic FAK expression is important for the morphogenetic events of gastrulation, neurulation, axial elongation and somitogenesis.

FAK morphant phenotypes are not due to disruption of Fn matrix

The defects in mesoderm development evident in FAK null mice (Furuta et al., 1995) are similar to both Fn (Georges-Labouesse et al., 1996) and integrin α5 nulls (Yang et al., 1993), suggesting a general role for cell–ECM interactions in this tissue. Indeed, loss of Fn in zebrafish (Jülich et al., 2005) or *Xenopus* (Davidson et al., 2006) leads to defects in blastopore closure, axial elongation and somitogenesis that are similar to those in FAK morphant embryos. The assembly of the Fn matrix in *Xenopus* embryos has been reported to regulate the rate of mesendoderm migration (Rozario et al., 2009). Could loss of Fn matrix account for the defects observed in the migration of mesendoderm in FAK morphant embryos? Previous work using FAK null cells in culture (Ilić et al., 2004) or expression of exogenous FRNK in *Xenopus* (Kragtorp and Miller, 2006) suggested that FAK may be an important factor in the assembly of Fn fibrils. Moreover, the progressive assembly of matrix during *Xenopus* gastrulation is dependent on tissue tension in the ectodermal cells of the blastocoel roof (Dzamba et al., 2009), so any changes in cell and tissue stresses at this stage might be expected to alter matrix assembly. However, we find no disruption of Fn matrix in FAK morphant embryos (Fig. S3B), nor was any significant disruption in matrix reported previously in embryos injected with FF (Petridou et al., 2013). We conclude that the fraction of $pFAK^{Y397}$ present in FAK morphant embryos (Fig. S3D) is sufficient to support assembly of Fn matrix on the blastocoel roof. We speculate that maternally expressed FAK is highly phosphorylated on Y397 possibly compensating for the loss of zygotic FAK in these embryos. These results suggest that defects in the migration of FAK deficient mesendoderm are not the consequence of a reduction in Fn matrix assembly along the blastocoel roof but rather a result of "tissue autonomous" changes in migratory capacity of the mesendoderm.

FAK is necessary for directed migration and protrusive activity

Our findings demonstrate that FAK is critical for persistent and directional migration of mesendoderm cells both in isolation and in intact tissue. Single FAK morphant mesendoderm cells migrate more slowly and erratically than control cells and cell spreading is decreased (Fig. 2, Fig. 6). The persistence of collectively migrating FAK morphant cells is also decreased and protrusive polarity severely disrupted. Furthermore, maintenance of cell–cell contacts and tissue geometry are alone not sufficient to generate directed migration in the absence of FAK. Control cells in explanted tissue, either on glass or on softer gel substrates, have significantly greater persistence than isolated cells. In contrast, FAK morphant cells do not exhibit increased persistence when part of an explant even on relatively soft substrates, which are more likely to be comparable to that encountered in vivo. The decreased persistence of FAK morphant cells may help explain the reduced migration rate reported following perturbation of FAK in *Xenopus* mesendoderm and other cell types (Petridou et al., 2013; Schlaepfer et al., 2004; Stylianou and Skourides, 2009).

Decreased persistence could be explained by changes in the stability of protrusions. We observed an increase in the number of lamellipodial protrusions in FAK morphant mesendoderm (Fig. 3 D), consistent with previous observations of cultured fibroblasts and macrophages (Owen et al., 2007; Tilghman et al., 2005). However, the broad lamellipodia evident in control mesendoderm cells are rarely observed in FAK morphant cells (Fig. 3A, B) or FAK null fibroblasts (Tilghman et al., 2005). Instead, FAK morphant cells exhibit multiple smaller protrusions with aberrant morphologies, suggesting that FAK is important for stabilization of broad lamellipodial protrusions at the leading edge of migrating cells. FAK has also been shown to facilitate the turnover of integrin adhesion complexes, and this is thought to be a key function of FAK in cell migration (Ilić et al., 1995; Owen et al., 2007; Ren et al., 2000; Schober et al., 2007). The off-axis protrusions observed in FAK morphant mesendoderm could therefore be the result of failure to disassemble adhesions and retract mis-directed protrusions. Thus, FAK may be acting at the leading edge to stabilize polarized protrusions and also at the lateral and trailing edges to tune polarity by facilitating turnover of adhesions in off-axis protrusions.

In addition to the increase in lamellipodial protrusions, we observed a marked increase in filopodia-like protrusions in FAK morphant tissues. The general morphology of these filopodial protrusions are similar to those observed in other FAK null cells (Ilić et al., 1995; Tilghman et al., 2005). The abundance of filopodia-like protrusions or microspikes is reminiscent of changes in Cdc42 signaling (Hall, 1998). It is well known that Rho family GTPases, including Rho, Rac, and Cdc42, are integral to regulation of adhesion and migration (Nobes and Hall, 1999). Both increases and decreases in Rho, Rac, or Cdc42 activity can have a dramatic impact on actin organization and the morphology of protrusions, and there have been several studies linking FAK to modulation of Rho GTPase signaling (Chang et al., 2007; Chen et al., 2002; Fabry et al., 2011; Lim et al., 2008; Myers et al., 2012; Ren et al., 2000; Tomar et al., 2009). Thus, modulation of Rho, Rac, or Cdc42 activity is a potential mechanism by which FAK may regulate protrusive morphology in the mesendoderm tissue and perhaps actin organization as well.

Reduced traction and spreading of FAK morphant cells disrupts actin and keratin organization

In control cells, actin filaments fill lamellipodial protrusions and form a fine cortical mesh while keratin filaments are biased toward the rear of each cell. FAK morphant cells have an increase in actin microspikes in protrusions and the appearance of actin stress fibers throughout the cell body. We also observe dense cortical actin bundles and other aberrant actin structures in rounded FAK morphant cells (data not shown), similar to the typical phenotype of FAK null fibroblasts (Fabry et al., 2011; Ilić et al., 1995; Serrels et al., 2007; Sieg et al., 1999). However, we find that in spread and polarized cells, a minority of the FAK morphant population, there is a more modest change in actin organization (Fig. 4). This suggests that large changes in actin organization often noted in the absence of FAK are not directly associated with cell polarity but more likely are related to cell spreading. Assembly and organization of the keratin filament network are thought to be dependent on actin (Kölsch et al., 2009; Wöll et al., 2005). Therefore, the changes in keratin organization in FAK morphant cells could be a result of alterations in the actin cytoskeleton. In FAK morphant cells, changes in actin are accompanied by a seemingly random organization of keratin filaments in each cell and the absence of keratin cabling along the leading edge of the tissue. Disruptions of the actin filament network are less severe than those of the keratin network and thus unlikely to account for the major alterations observed in keratin filament organization.

How might FAK affect the organization of keratin filaments, if not via changes in the actin network? We noted a marked similarity between the appearance of keratin filaments in many of the FAK morphant cells and in control cells plated on poly-L-lysine. Mesendoderm cells attach tightly to poly-L-lysine substrates but fail to generate significant traction forces under these conditions. The cells do not spread and the keratin filaments exhibit a "wagon wheel" arrangement (Weber et al., 2012). This

same arrangement is observed in FAK morphant cells, which also spread poorly (Figs. 5C and 6B). FAK is thought to regulate cell spreading via activation of integrins and regulation of adhesion turnover (Michael et al., 2009; Mitra et al., 2005; Ren et al., 2000). FAK morphant cells exert less traction force on Fn substrates (Fig. 6C) and this decrease in traction force per cell is correlated with reduced spreading (Fig. S5) as previously reported for FAK null fibroblasts (Fabry et al., 2011). Both traction on Fn and tugging forces on cadherin adhesions contribute to the normal spatial organization of keratin filaments within mesendoderm cells (Weber et al., 2012). In addition integrin α5β1 is required for the development of anisotropic tension in the mesendoderm (Davidson et al., 2002). Therefore, FAK may be regulating keratin organization indirectly by facilitating the generation of the traction forces on Fn required for spreading and for development of anisotropic tension by integrins within the migrating tissue.

We reported previously that coordinated protrusive activity in the mesendoderm is dependent on tugging forces on cadherins, recruitment of plakoglobin (γ-catenin), and reorganization of keratin filaments (Weber et al., 2012). Interestingly, the disruption of tissue polarity in FAK morphant embryos is similar to that observed in keratin morphants. However, both keratin organization and tissue polarity are more severely affected by depletion of FAK than by loss of plakoglobin. Protrusive polarity is significantly disrupted in both leading and following cells in FAK morphant tissue, in contrast to the subtle changes in directional distribution of protrusions in plakoglobin morphant tissue. Moreover, plakoglobin morphant mesendoderm maintains a continuous leading edge with keratin cables running perpendicular to the direction of travel while FAK morphant mesendoderm has a discontinuous leading edge and lacks these cables. Loss of directional and persistent migration could cause the discontinuity of the leading edge observed in both in FAK morphant mesendoderm (Fig. 3B) and in FAK null fibroblasts (Tilghman et al., 2005) and may result in an inability to form trans-cellular cabling. If supra-cellular organization of keratin or other cytoskeletal elements serves to maintain or reinforce tissue polarity, the lack of such structures in FAK morphants would account for the increased disruption of tissue polarity relative to plakoglobin morphants, particularly at the leading edge.

FAK is required for efficient assembly of a mechanoresponsive cadherin adhesion complex

One intriguing finding is the decreased association of plakoglobin with C-cadherin in FAK morphant embryos during the period of development when tissue polarity is established (Fig. 7). One possible explanation for the effect of FAK on plakoglobin–cadherin association is a change in cellular contractility. FAK can modulate acto-myosin contractility via Rho and Rho-kinase (Fabry et al., 2011; Playford et al., 2008; Ren et al., 2000; Schober et al., 2007) and cellular contractility affects stability of cadherin adhesions(Braga and Yap, 2005; Liu et al., 2010; Playford et al., 2008; Yamada and Nelson, 2007), traction forces on Fn (Beningo et al., 2006), and organization of the actin cytoskeleton (Burridge and Wennerberg, 2004; Hall, 1998). We observed no change in phosphorylation of myosin light chain in FAK morphants (Fig. S4), but it is possible that FAK is regulating cellular contractility via another signaling pathway.

What other factors might explain the role of FAK in assembly of the mechanoresponsive cadherin complex? We noted a decrease in association of plakoglobin with C-cadherin that is dependent on developmental stage; by the end of gastrulation there is no difference between FAK morphants and controls (Fig. 7). FAK knockdown has no effect on association of β-catenin with C-cadherin (Fig. 7), an interaction previously reported to increase at the onset of gastrulation (Schneider et al., 1993). We speculate that delays and defects in FAK morphant mesendoderm migration per se reflect a decrease in anisotropic mechanical stimulation of cadherin adhesions and thereby inefficient assembly of the cadherin–plakoglobin–keratin complex that is required for coordination of migration (Weber et al., 2012).

In summary, these data suggest that FAK has an essential role in governing the organization of morphogenetic movements during early development. FAK may be working to regulate substrate tractions (via integrins) and thereby maintain a balance of forces between traction and cell–cell cohesion (via cadherins) that is critical for self-organization and directionality of migrating mesendoderm. Loss of this organization in vivo results in defects in the development of the anterior and dorsal structures to which the mesendoderm contributes. It is clear that coordination of collective cell migration depends on both cadherin and integrin adhesion complexes, though the specific mechanisms of interaction between these adhesions have yet to be fully elucidated. A key area of interest is the mechanism by which signals are transduced between the mechanoresponsive cadherin adhesions at the rear and lateral sides of the cell and the integrin-based adhesions at the front of the cell. How mechanical signals are transduced by cells also remains poorly understood. Recent work suggests this could occur through force-induced conformational changes (Johnson et al., 2007; Sawada et al., 2006), particularly in proteins associated with adhesions (e.g. Yonemura et al., 2010). Emerging methodologies (Borghi et al., 2012; Eyckmans et al., 2011; Grashoff et al., 2010; Legant et al., 2010; Machacek et al., 2009) will allow these questions to be addressed with the high degree of spatial and temporal resolution required for understanding of the complex and dynamic signals likely to be involved. Further studies will be needed to enhance our understanding of the adhesive networks that transduce chemical and mechanical signals important in the collective cell movements essential for development.

Acknowledgments

We thank Christopher Chen, Michael Yang and Mark Breckenridge for microfabricated post array detectors (mPADs), Matlab analysis module and assistance with troubleshooting. We also thank Shayn Peirce-Cottler, Joseph Walpole and Angela Jividen for assistance with analysis of traction data. We extend our gratitude to colleague Gregory Weber for helpful discussions over the course of these studies, to Glen Bjerke, Glen Hirsh and especially Ann Sutherland for critical reading of the manuscript, to Fred Simon for excellent animal care, and to all the investigators who provided reagents. This work was supported by USPHS grants T32-GM08136 to M.A.B. and R01-HD26402/GM094793 and R21-HD071136 to D.W.D.

Appendix A. Supporting information

Supplementary data associated with this article can be found in the online version at http://dx.doi.org/10.1016/j.ydbio.2014.07.023.

References

Beningo, K.A., Hamao, K., Dembo, M., Wang, Y.-L., Hosoya, H., 2006. Traction forces of fibroblasts are regulated by the Rho-dependent kinase but not by the myosin light chain kinase. Arch. Biochem. Biophys. 456, 224–231.

Borghi, N., Sorokina, M., Shcherbakova, O.G., Weis, W.I., Pruitt, B.L., Nelson, W.J., Dunn, A.R., 2012. E-cadherin is under constitutive actomyosin-generated tension that is increased at cell–cell contacts upon externally applied stretch. Proc. Natl. Acad. Sci. U.S.A 109, 12568–12573.

Braga, V.M.M., Yap, A.S., 2005. The challenges of abundance: epithelial junctions and small GTPase signalling. Curr. Opin. Cell Biol. 17, 466–474.

Brieher, W.M., Gumbiner, B.M., 1994. Regulation of C-cadherin function during activin induced morphogenesis of animal caps. J. Cell Biol. 126, 519–527.
Burridge, K., Wennerberg, K., 2004. Rho and Rac take center stage. Cell 116, 167–179.
Butler, J.P., Tolić-Nørrelykke, I.M., Fabry, B., Fredberg, J.J., 2002. Traction fields, moments, and strain energy that cells exert on their surroundings. Am. J. Physiol. Cell Physiol. 282, C595–C605.
Calalb, M.B., Polte, T.R., Hanks, S.K., 1995. Tyrosine phosphorylation of focal adhesion kinase at sites in the catalytic domain regulates kinase activity: a role for Src family kinases. Mol. Cell. Biol. 15, 954–963.
Chang, F., Lemmon, C.A., Park, D., Romer, L.H., 2007. FAK potentiates Rac1 activation and localization to matrix adhesion sites: a role for βPIX. Mol. Biol. Cell 18, 253–264.
Chen, B.-H., Tzen, J.T.C., Bresnick, A.R., Chen, H.-C., 2002. Roles of Rho-associated kinase and myosin light chain kinase in morphological and migratory defects of focal adhesion kinase-null cells. J. Biol. Chem. 277, 33857–33863.
Clarke, E.J., Allan, V.J., 2003. Cytokeratin intermediate filament organisation and dynamics in the vegetal cortex of living Xenopus laevis oocytes and eggs. Cell Motil. Cytoskelet. 56, 13–26.
Crawford, B.D., Henry, C.A., Clason, T.A., Becker, A.L., Hille, M.B., 2003. Activity and distribution of paxillin, focal adhesion kinase, and cadherin indicate cooperative roles during zebrafish morphogenesis. Mol. Biol. Cell 14, 3065–3081.
Davidson, L.A., Hoffstrom, B.G., Keller, R., DeSimone, D.W., 2002. Mesendoderm extension and mantle closure in Xenopus laevis gastrulation: combined roles for integrin α5β1, fibronectin, and tissue geometry. Dev. Biol. 242, 109–129.
Davidson, L.A., Keller, R., DeSimone, D.W., 2004. Patterning and tissue movements in a novel explant preparation of the marginal zone of Xenopus laevis. Gene Expr. Patterns 4, 457–466.
Davidson, L.A., Marsden, M., Keller, R., DeSimone, D.W., 2006. Integrin α5β1 and fibronectin regulate polarized cell protrusions required for Xenopus convergence and extension. Curr. Biol. 16, 833–844.
Dimitriadis, E.K., Horkay, F., Maresca, J., Kachar, B., Chadwick, R.S., 2002. Determination of elastic moduli of thin layers of soft material using the atomic force microscope. Biophys. J. 82, 2798–2810.
Doherty, J.T., Conlon, F.L., Mack, C.P., Taylor, J.M., 2010. Focal adhesion kinase is essential for cardiac looping and multichamber heart formation. Genesis 48, 492–504.
Dumbauld, D.W., Shin, H., Gallant, N.D., Michael, K.E., Radhakrishna, H., García, A.J., 2010. Contractility modulates cell adhesion strengthening through focal adhesion kinase and assembly of vinculin-containing focal adhesions. J. Cell. Physiol. 223, 746–756.
Dzamba, B.J., Jakab, K.R., Marsden, M., Schwartz, M.A., DeSimone, D.W., 2009. Cadherin adhesion, tissue tension, and noncanonical Wnt signaling regulate fibronectin matrix organization. Dev. Cell 16, 421–432.
Eyckmans, J., Boudou, T., Yu, X., Chen, C.S., 2011. A hitchhiker's guide to mechanobiology. Dev. Cell 21, 35–47.
Fabry, B., Klemm, A.H., Kienle, S., Schäffer, T.E., Goldmann, W.H., 2011. Focal adhesion kinase stabilizes the cytoskeleton. Biophys. J. 101, 2131–2138.
Fonar, Y., Gutkovich, Y.E., Root, H., Malyarova, A., Aamar, E., Golubovskaya, V.M., Elias, S., Elkouby, Y.M., Frank, D., 2011. Focal adhesion kinase protein regulates Wnt3a gene expression to control cell fate specification in the developing neural plate. Mol. Biol. Cell 22, 2409–2421.
Furuta, Y., Ilić, D., Kanazawa, S., Takeda, N., Yamamoto, T., Aizawa, S., 1995. Mesodermal defect in late phase of gastrulation by a targeted mutation of focal adhesion kinase, FAK. Oncogene 11, 1989–1995.
Georges-Labouesse, E., George, E.L., Rayburn, H., Hynes, R.O., 1996. Mesodermal development in mouse embryos mutant for fibronectin. Dev. Dyn. 207, 145–156.
Grashoff, C., Hoffman, B.D., Brenner, M.D., Zhou, R., Parsons, M., Yang, M.T., McLean, M.A., Sligar, S.G., Chen, C.S., Ha, T., Schwartz, M.A., 2010. Measuring mechanical tension across vinculin reveals regulation of focal adhesion dynamics. Nature 466, 263–266.
Gu, J., Tamura, M., Pankov, R., Danen, E.H.J., Takino, T., Matsumoto, K., Yamada, K.M., 1999. Shc and FAK differentially regulate cell motility and directionality modulated by PTEN. J. Cell Biol. 146, 389–403.
Hall, A., 1998. Rho GTPases and the actin cytoskeleton. Science 279, 509–514.
Hammer, Ø., Harper, D.A.T., Ryan, P.D., 2001. PAST: Paleontological statistics software package for education and data analysis. Palaeontol. Electron. 4, 1–9.
Hanks, S.K., Calalb, M.B., Harper, M.C., Patel, S.K., 1992. Focal adhesion protein-tyrosine kinase phosphorylated in response to cell attachment to fibronectin. Proc. Natl. Acad. Sci. U.S.A 89, 8487–8491.
Henry, C.A., Crawford, B.D., Yan, Y.-L., Postlethwait, J., Cooper, M.S., Hille, M.B., 2001. Roles for zebrafish focal adhesion kinase in notochord and somite morphogenesis. Dev. Biol. 240, 474–487.
Hens, M.D., DeSimone, D.W., 1995. Molecular analysis and developmental expression of the focal adhesion kinase pp125FAK in Xenopus laevis. Dev. Biol. 170, 274–288.
Ilić, D., Furuta, Y., Kanazawa, S., Takeda, N., Sobue, K., Nakatsuji, N., Nomura, S., Fujimoto, J., Okada, M., Yamamoto, T., Aizawa, S., 1995. Reduced cell motility and enhanced focal adhesion contact formation in cells from FAK-deficient mice. Nature 377, 539–544.
Ilić, D., Kovacic, B., Johkura, K., Schlaepfer, D.D., Tomasević, N., Han, Q., Kim, J.-B., Howerton, K., Baumbusch, C., Ogiwara, N., Streblow, D.N., Nelson, J.A., Dazin, P., Shino, Y., Sasaki, K., Damsky, C.H., 2004. FAK promotes organization of fibronectin matrix and fibrillar adhesions. J. Cell Sci. 117, 177–187.
Johnson, C.P., Tang, H.-Y., Carag, C., Speicher, D.W., Discher, D.E., 2007. Supplement: forced unfolding of proteins within cells. Science 317, 663–666.
Jülich, D., Geisler, R., Holley, S.A., 2005. Integrin α5 and delta/notch signaling have complementary spatiotemporal requirements during zebrafish somitogenesis. Dev. Cell 8, 575–586.
Keller, R., 2002. Shaping the vertebrate body plan by polarized embryonic cell movements. Science 298, 1950–1954.
Keller, R., 2012. Physical biology returns to morphogenesis. Science 338, 201–203.
Keller, R., Danilchik, M., 1988. Regional expression, pattern and timing of convergence and extension during gastrulation of Xenopus laevis. Development 103, 193–209.
Keller, R., Davidson, L.A., Edlund, A., Elul, T., Ezin, M., Shook, D., Skoglund, P., 2000. Mechanisms of convergence and extension by cell intercalation. Philos. Trans. R. Soc. Lond. B. Biol. Sci. 355, 897–922.
Kölsch, A., Windoffer, R., Leube, R.E., 2009. Actin-dependent dynamics of keratin filament precursors. Cell Motil. Cytoskelet. 66, 976–985.
Kragtorp, K.A., Miller, J.R., 2006. Regulation of somitogenesis by Ena/VASP proteins and FAK during Xenopus development. Development 133, 685–695.
Lee, C.-H., Gumbiner, B.M., 1995. Disruption of gastrulation movements in Xenopus by a dominant-negative mutant for C-cadherin. Dev. Biol. 171, 363–373.
Legant, W.R., Miller, J.S., Blakely, B.L., Cohen, D.M., Genin, G.M., Chen, C.S., 2010. Measurement of mechanical tractions exerted by cells in three-dimensional matrices. Nat. Methods 7, 969–971.
Lim, S.-T., Chen, X.L., Tomar, A., Miller, N.L.G., Yoo, J., Schlaepfer, D.D., 2010. Knock-in mutation reveals an essential role for focal adhesion kinase activity in blood vessel morphogenesis and cell motility-polarity but not cell proliferation. J. Biol. Chem. 285, 21526–21536.
Lim, Y., Lim, S.-T., Tomar, A., Gardel, M.L., Bernard-Trifilo, J.A., Chen, X.L., Uryu, S.A., Canete-Soler, R., Zhai, J., Lin, H., Schlaepfer, W.W., Nalbant, P., Bokoch, G., Ilić, D., Waterman-Storer, C.M., Schlaepfer, D.D., 2008. PyK2 and FAK connections to p190Rho guanine nucleotide exchange factor regulate RhoA activity, focal adhesion formation, and cell motility. J. Cell Biol. 180, 187–203.
Liu, Z., Tan, J.L., Cohen, D.M., Yang, M.T., Sniadecki, N.J., Ruiz, S.A., Nelson, C.M., Chen, C.S., 2010. Mechanical tugging force regulates the size of cell-cell junctions. Proc. Natl. Acad. Sci. U.S.A 107, 9944–9949.
Machacek, M., Hodgson, L., Welch, C., Elliott, H., Pertz, O., Nalbant, P., Abell, A., Johnson, G.L., Hahn, K.M., Danuser, G., 2009. Coordination of Rho GTPase activities during cell protrusion. Nature 461, 99–103.
Marsden, M., DeSimone, D.W., 2001. Regulation of cell polarity, radial intercalation and epiboly in Xenopus: novel roles for integrin and fibronectin. Development 128, 3635–3647.
Marsden, M., DeSimone, D.W., 2003. Integrin-ECM interactions regulate cadherin-dependent cell adhesion and are required for convergent extension in Xenopus. Curr. Biol. 13, 1182–1191.
Michael, K.E., Dumbauld, D.W., Burns, K.L., Hanks, S.K., García, A.J., 2009. FAK modulates cell adhesion strengthening via integrin activation. Mol. Biol. Cell 20, 2508–2519.
Mitra, S.K., Hanson, D.A., Schlaepfer, D.D., 2005. Focal adhesion kinase: in command and control of cell motility. Nat. Rev. Mol. Cell Biol. 6, 56–68.
Myers, J.P., Robles, E., Ducharme-Smith, A., Gomez, T.M., 2012. Focal adhesion kinase modulates Cdc42 activity downstream of positive and negative axon guidance cues. J. Cell Sci. 125, 2918–2929.
Nieuwkoop, P.D., Faber, J., 1994. Normal Table of Xenopus laevis (Daudin). Garland Publishing Inc, New York.
Ninomiya, H., Elinson, R.P., Winklbauer, R., 2004. Antero-posterior tissue polarity links mesoderm convergent extension to axial patterning. Nature 430, 364–367.
Nobes, C.D., Hall, A., 1999. Rho GTPases control polarity, protrusion, and adhesion during cell movement. J. Cell Biol. 144, 1235–1244.
Owen, K.A., Pixley, F.J., Thomas, K.S., Vicente-Manzanares, M., Ray, B.J., Horwitz, A.F., Parsons, J.T., Beggs, H.E., Stanley, E.R., Bouton, A.H., 2007. Regulation of lamellipodial persistence, adhesion turnover, and motility in macrophages by focal adhesion kinase. J. Cell Biol. 179, 1275–1287.
Parsons, J.T., 2003. Focal adhesion kinase: the first ten years. J. Cell Sci. 116, 1409–1416.
Petridou, N.I., Stylianou, P., Christodoulou, N., Rhoads, D., Guan, J.-L., Skourides, P.A., 2012. Activation of endogenous FAK via expression of its amino terminal domain in Xenopus embryos. PLoS One 7, e42577.
Petridou, N.I., Stylianou, P., Skourides, P.A., 2013. A dominant-negative provides new insights into FAK regulation and function in early embryonic morphogenesis. Development 140, 4266–4276.
Playford, M.P., Vadali, K., Cai, X., Burridge, K., Schaller, M.D., 2008. Focal adhesion kinase regulates cell–cell contact formation in epithelial cells via modulation of Rho. Exp. Cell Res. 314, 3187–3197.
Rajagopalan, P., Marganski, W. a, Brown, X.Q., Wong, J.Y., 2004. Direct comparison of the spread area, contractility, and migration of balb/c 3T3 fibroblasts adhered to fibronectin- and RGD-modified substrata. Biophys. J. 87, 2818–2827.
Ramos, J.W., Whittaker, C.A., DeSimone, D.W., 1996. Integrin-dependent adhesive activity is spatially controlled by inductive signals at gastrulation. Development 122, 2873–2883.
Ren, X.-D., Kiosses, W.B., Sieg, D.J., Otey, C.A., Schlaepfer, D.D., Schwartz, M.A., 2000. Focal adhesion kinase suppresses Rho activity to promote focal adhesion turnover. J. Cell Sci. 113, 3673–3678.
Rozario, T., Dzamba, B.J., Weber, G.F., Davidson, L.A., DeSimone, D.W., 2009. The physical state of fibronectin matrix differentially regulates morphogenetic movements in vivo. Dev. Biol. 327, 386–398.
Sawada, Y., Tamada, M., Dubin-Thaler, B.J., Cherniavskaya, O., Sakai, R., Tanaka, S., Sheetz, M.P., 2006. Force sensing by mechanical extension of the Src family kinase substrate p130Cas. Cell 127, 1015–1026.

Schaller, M.D., Borgman, C.A., Cobb, B.S., Vines, R.R., Reynolds, A.B., Parsons, J.T., 1992. pp125FAK a structurally distinctive protein-tyrosine kinase associated with focal adhesions. Proc. Natl. Acad. Sci. U.S.A 89, 5192–5196.
Schindelin, J., Arganda-Carreras, I., Frise, E., Kaynig, V., Longair, M., Pietzsch, T., Preibisch, S., Rueden, C., Saalfeld, S., Schmid, B., Tinevez, J.-Y., White, D.J., Hartenstein, V., Eliceiri, K., Tomancak, P., Cardona, A., 2012. Fiji: an open-source platform for biological-image analysis. Nat. Methods 9, 676–682.
Schlaepfer, D.D., Hauck, C.R., Sieg, D.J., 1999. Signaling through focal adhesion kinase. Prog. Biophys. Mol. Biol. 71, 435–478.
Schlaepfer, D.D., Mitra, S.K., Ilić, D., 2004. Control of motile and invasive cell phenotypes by focal adhesion kinase. Biochim. Biophys. Acta 1692, 77–102.
Schneider, S., Herrenknecht, K., Butz, S., Kemler, R., Hausen, P., 1993. Catenins in Xenopus embryogenesis and their relation to the cadherin-mediated cell–cell adhesion system. Development 118, 629–640.
Schober, M., Raghavan, S., Nikolova, M., Polak, L., Pasolli, H.A., Beggs, H.E., Reichardt, L.F., Fuchs, E., 2007. Focal adhesion kinase modulates tension signaling to control actin and focal adhesion dynamics. J. Cell Biol. 176, 667–680.
Schwartz, M.A., DeSimone, D.W., 2008. Cell adhesion receptors in mechanotransduction. Curr. Opin. Cell Biol. 20, 551–556.
Serrels, B., Serrels, A., Brunton, V.G., Holt, M., McLean, G.W., Gray, C.H., Jones, G.E., Frame, M.C., 2007. Focal adhesion kinase controls actin assembly via a FERM-mediated interaction with the Arp2/3 complex. Nat. Cell Biol. 9, 1046–1056.
Shook, D., Keller, R., 2003. Mechanisms, mechanics and function of epithelial–mesenchymal transitions in early development. Mech. Dev. 120, 1351–1383.
Sieg, D.J., Hauck, C.R., Schlaepfer, D.D., 1999. Required role of focal adhesion kinase (FAK) for integrin-stimulated cell migration. J. Cell Sci. 112, 2677–2691.
Sive, H.L., Grainger, R.M., Harland, R.M., 2000. Early development of Xenopus laevis: a laboratory manual. Cold Spring Harbor Laboratory Press, Cold Spring Harbor, NY.
Stylianou, P., Skourides, P.A., 2009. Imaging morphogenesis, in Xenopus with quantum dot nanocrystals. Mech. Dev. 126, 828–841.
Symes, K., Smith, J.C., 1987. Gastrulation movements provide an early marker of mesoderm induction in Xenopus laevis. Development 101, 339–349.
Tilghman, R.W., Slack-Davis, J.K., Sergina, N., Martin, K.H., Iwanicki, M., Hershey, E. D., Beggs, H.E., Reichardt, L.F., Parsons, J.T., 2005. Focal adhesion kinase is required for the spatial organization of the leading edge in migrating cells. J. Cell Sci. 118, 2613–2623.
Tomar, A., Lim, S.-T., Lim, Y., Schlaepfer, D.D., 2009. A FAK-p120RasGAP-p190RhoGAP complex regulates polarity in migrating cells. J. Cell Sci. 122, 1852–1862.
Tseng, Q., Duchemin-Pelletier, E., Deshiere, A., Balland, M., Guillou, H., Filhol, O., Théry, M., 2012. Spatial organization of the extracellular matrix regulates cell-cell junction positioning. Proc. Natl. Acad. Sci. U.S.A 109, 1506–1511.
Wang, H., Radjendirane, V., Wary, K.K., Chakrabarty, S., 2004. Transforming growth factor β regulates cell–cell adhesion through extracellular matrix remodeling and activation of focal adhesion kinase in human colon carcinoma Moser cells. Oncogene 23, 5558–5561.
Wang, H.-B., Dembo, M., Hanks, S.K., Wang, Y.-L., 2001. Focal adhesion kinase is involved in mechanosensing during fibroblast migration. Proc. Natl. Acad. Sci. U.S.A 98, 11295–11300.
Weber, G.F., Bjerke, M.A., DeSimone, D.W., 2011. Integrins and cadherins join forces to form adhesive networks. J. Cell Sci. 124, 1183–1193.
Weber, G.F., Bjerke, M.A., DeSimone, D.W., 2012. A mechanoresponsive cadherin–keratin complex directs polarized protrusive behavior and collective cell migration. Dev. Cell 22, 104–115.
Winklbauer, R., 2009. Cell adhesion in amphibian gastrulation. Int. Rev. Cell Mol. Biol. 278, 215–275.
Wöll, S., Windoffer, R., Leube, R.E., 2005. Dissection of keratin dynamics: different contributions of the actin and microtubule systems. Eur. J. Cell Biol. 84, 311–328.
Wozniak, M.A., Chen, C.S., 2009. Mechanotransduction in development: a growing role for contractility. Nat. Rev. Mol. Cell Biol. 10, 34–43.
Yamada, S., Nelson, W.J., 2007. Localized zones of Rho and Rac activities drive initiation and expansion of epithelial cell–cell adhesion. J. Cell Biol. 178, 517–527.
Yang, J.T., Rayburn, H., Hynes, R.O., 1993. Embryonic mesodermal defects in α5 integrin-deficient mice. Development 119, 1093–1105.
Yang, M.T., Fu, J., Wang, Y.-K., Desai, R.A., Chen, C.S., 2011. Assaying stem cell mechanobiology on microfabricated elastomeric substrates with geometrically modulated rigidity. Nat. Protoc. 6, 187–213.
Yonemura, S., Wada, Y., Watanabe, T., Nagafuchi, A., Shibata, M., 2010. α-Catenin as a tension transducer that induces adherens junction development. Nat. Cell Biol. 12, 533–542.